Towards Reliable Modeling of S-Nitrosothiol Chemistry: Explicitly-Correlated Coupled Cluster and DFT Studies

Dmitry Khomyakov
Marquette University

TOWARDS RELIABLE MODELING OF S-NITROSOTHIOL CHEMISTRY: EXPLICITLY-CORRELATED COUPLED CLUSTER AND DFT STUDIES

by

Dmitry G. Khomyakov, MSc.

A Thesis submitted to the Faculty of the Graduate School,

Marquette University,

in Partial Fulfillment of the Requirements for

the Degree of Master of Science

Milwaukee, Wisconsin

May 2015

ABSTRACT
TOWARDS RELIABLE MODELING OF S-NITROSOTHIOL CHEMISTRY:
EXPLICITLY-CORRELATED COUPLED CLUSTER AND DFT STUDIES

Dmitry G. Khomyakov, MSc.

Marquette University, 2015

In this work, we apply recently proposed explicitly-correlated coupled cluster methods, CCSD(T)-F12x, as well as density functional theory methods, to study the acid-base properties of HSNO molecule in gas phase. Used in this work approach theoretical efficiently alleviates excessive computational cost of the traditional *ab initio* methods, used in computational chemistry, with identical level of accuracy.

Our high-level reference calculations show that protonation of HSNO molecule will most readily occur at the S atom (with energy release ~ 17 kcal/mol), compared to N atom (energy release ~ 5 kcal/mol) or O atom (energy release ~ 7 kcal/mol). S–N bond in HSNO elongates by 0.572 Å and weakens by 11.1 kcal/mol upon protonation at the S atom, gaining noticeable anharmonic character. Deprotonation of HSNO is thermodynamically unfavorable, with energy loss ~ 170 kcal/mol, accompanied with S-N bond shortening by 0.149 Å.

Based on generated in this work the reference values, we tested and ranked the performance of total 45 different DFT functionals of various families and rungs of the DFT "Jacob's ladder", applied to HSNO in neutral or protonated and deprotonated forms. Best performing functionals are identified for the future computational studies of the biologically relevant reactions involving S-nitrosothiols.

TABLE OF CONTENTS

LIST OF ABBREVIATIONS

BDE – bond dissociation energy

CBS – complete basis set

CCSD – coupled cluster method with single and double excitations

CCSD(T) – coupled cluster method with single, double and triple excitations

CV – core-valence

DFT – density functional theory

GGA – general gradient approximation

HF – Hartree-Fock

LA – Lewis Acid

MAD – maximum absolute deviation

PES – potential energy surface

QM/MM – quantum mechanics/molecular mechanics

RMSD – root mean-square deviation

TS – transition state

ZPE – zero-point energy

Introduction

The biological importance of S-nitrosothiols (RSNOs), relatively unstable derivatives of thiols (RSH), is increasingly coming into focus in the life sciences (Anand, Hess, & Stamler, 2013; Cox et al., 2014; Haldar & Stamler, 2013). S-Nitrosated cysteine residues in peptides and proteins act as storage pool of nitric oxide NO, a major gasotrasmitter, and the regulated S-nitrosation/denitrosation of specific cysteine residues in proteins is involved in a multitude of key biological processes across all branches of the tree of life (Anand & Stamler, 2012; Hess & Stamler, 2012), from immune response in plants to neurotransmission in humans. Moreover, the smallest RSNO—thionitrous acid HSNO—has been recently proposed to be a short-lived endogenous biological species involved in signaling processes (Bruce King 2012; Filipovic et al., 2012; Miljkovic et al., 2013).

Although the ubiquity of regulated biological RSNO reactions is now well established, the atomic-level mechanisms underlying the precise enzymatic control of these processes are yet to be uncovered. However, recent theoretical considerations of the complex and unique electronic structure of the –SNO group have shown that RSNO reactivity can be dramatically altered by interaction with Lewis acids, suggesting a wide range of possibilities for specific/general acid and metal-ion catalytic control of RSNO reactions (Baciu & Gauld, 2003; Moran, Timerghazin, Kwong, & English, 2011; Perissinotti, Estrin, Leitus, & Doctorovich, 2006; Talipov & Timerghazin, 2013; Talipov, Khomyakov, Xian, & Timerghazin, 2013; Timerghazin, Peslherbe, & English, 2007).

The highly efficient modulation of the RSNO properties by Lewis acid coordination is due to the two antagonistic (Talipov & Timerghazin, 2013) resonance structures contributing into the overall electronic structure of the –SNO group—the zwitterionic and ionic structures with opposite bonding patterns and opposite formal charge distributions (Scheme 1). A coordinated Lewis acid changes the balance between the two antagonistic components and thus changes the RSNO reactivity: S-coordination promotes the ionic component and thus should catalyze N-atom directed nucleophilic attack/NO+ transfer, whereas O- and N-coordination should promote S-atom directed nucleophilic attack (Moran et al., 2011; Timerghazin & Talipov, 2013). In biologically relevant reactions with thiols, the former mechanism may be behind the puzzling selectivity of S-nitrosation in vivo (Doulias et al., 2010; Raju, Doulias, Tenopoulou, Greene, & Ischiropoulos, 2012), whereas the latter may result in formation of disulfide bridges and production of nitroxyl HNO—an elusive, yet highly potent bioactive species of pharmacological interest (Heinrich et al., 2013).

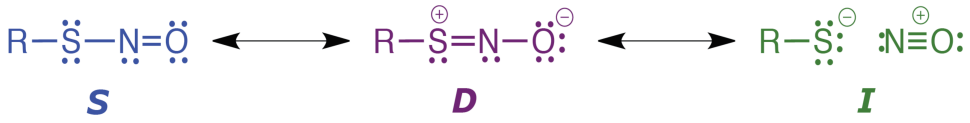

Scheme 1. Resonance description of the electronic structure of S-nitrosothiols.

Thus, the processes where RSNO acts as a base, e.g. protonation and coordination of charged aminoacid residues and/or metal centers, may play a crucial role in enzymatic control of the biological processes involving RSNOs (Talipov & Timerghazin, 2013), and also may be used in designing much needed efficient RSNO labeling reagents (Talipov et al., 2013). In addition, HSNO can also act as an acid by donating its proton and produc-

ing SNO– anion that may have its own distinct biochemistry. Accordingly, qualitative and quantitative understanding of the fundamental acid-base properties of organic RSNOs and HSNO is central for the further progress in the field.

Being rather unstable—the S–N bond dissociation energy is ~30 kcal/mol (Bartberger et al., 2001) —RSNOs can be challenging to study experimentally, which makes accurate computational predictions of the RSNO acid-base and other properties especially valuable. Unfortunately, accurate computational evaluation of the acid-base properties of RSNOs is also challenging at the moment due to several reasons, including a slow convergence of *ab initio* calculations with respect to the one- and multi-electron basis set size, inconsistent performance of DFT methods, and a significant anharmonicity of the –SNO group.

The S–N bond in RSNOs does not easily lend itself to accurate modeling using many conventional electronic structure methods. Indeed, the first comprehensive assessment by Baciu and Gauld (Baciu & Gauld, 2003) has shown a huge variation of calculated S–N bond lengths and dissociation energies depending on the model chemistry used; for instance, BDE(S–N) varied within >17 kcal/mol, with some model chemistries such as QCISD/6-311G giving decidedly unreasonable values of <16 kcal/mol.

Systematic coupled-cluster investigations (Ivanova, Anton, & Timerghazin, 2014; Timerghazin, Peslherbe, & English, 2008) shown that the S–N bond properties in RSNOs converge very slowly both with respect to the single-electron basis set size and the coupled-cluster excitation level, i.e. the multi-electron basis set size. As such, the minimal model required for RSNOs is coupled cluster with double and triple excitations extrapo-

lated to the complete basis set limit CCSD(T)/CBS, preferably with a correction for the quadruple excitations ΔQ (2014). Thus, obtaining reliable *ab inito* data on the RSNO properties and especially their reactivity is very taxing computationally, even for small RSNOs.

Although a number of DFT methods have shown some promise (Becke 2014; Burke 2012; Klimeš & Michaelides, 2012), their performance in the case of RSNO properties and reactivity is hard to assess due to the lack of high-quality reference *ab initio* or experimental data. Moreover, given the extreme malleability of the S–N bonding in RSNOs, whose nature can be dramatically modified by protonation/interaction with Lewis acids, a truly reliable DFT model chemistry should be able to consistently reproduce the S–N bond properties in all bonding regimes.

Another factor that may affect the accuracy of the calculated RSNO reaction energetics is the anharmonicity of the S–N bond, which is much floppier than typical covalent bonds: in HSNO, the calculated harmonic S–N stretch frequency is only ~350 cm^{-1} at the CCSD(T)/AVQZ level (Ivanova et al., 2014). As the S–N bond nature can dramatically change in chemical reactions and/or due to coordination, the zero-point vibrational energy (ZPE) has a significant contribution to the RSNO reaction thermochemistry (2014). The floppy bonds are also less harmonic, so the anharmonicity effects may have a non-negligible effect on the ZPE, which adds another layer of complexity to computational investigation of RSNO reactivity, given the computational burden associated with anharmonic frequency calculations.

Fortunately, the last decade has seen a dramatic progress in the development of the explicitly-correlated (F12) coupled-cluster techniques that dramatically accelerate the one-electron basis set convergence (Adler, Knizia, & Werner, 2007; Hill, Peterson, Knizia, & Werner, 2009; Knizia, Adler, & Werner, 2009). F12 methods augment the coupled-cluster expansion with terms that explicitly include the pairwise electron-electron distances r_{12}, usually in the form of Slater geminals $f_{12}=\exp(-r_{12})$, which effectively model the Coulomb hole around an electron. Recent methodological developments dramatically decreased the computational overhead due to the F12 terms; in particular, the CCSD(T)-F12x methods introduced by Werner and co-workers are only marginally more computationally demanding than the conventional coupled-cluster calculations (Knizia et al., 2009). These CCSD-F12a, CCSD-F12b (2009), and a very recently proposed CCSD-F12c (Martin & Kesharwani, 2014) approximations provide a hierarchy of methods with increasing number of the coupling terms between the conventional and explicitly-correlated terms of the coupled cluster expansion.

In general, the approximate F12 approaches depend on a large number of parameters and the construction of the auxiliary basis sets. However, CCSD-F12x and CCSD(T)-F12x now can be used as black-box 'model chemistry' electronic structure methods thanks to their efficient implementation with carefully chosen parameters in the Molpro code (Werner, Knowles, Knizia, Manby, & Schütz, 2012), and the development of the specialized basis set families along with the corresponding auxiliary F12 basis sets.

Accelerated one-electron basis set convergence of the F12x approaches, which usually demonstrate “two-zeta gain” over the conventional methods (Adler et al., 2007; Marchetti & Werner, 2008; Martin & Kesharwani, 2014), can be extremely useful to

overcome the excruciatingly slow basis set convergence of the computed RSNO properties (Hochlaf, Linguerri, & Francisco, 2013). However, given the complexity of the F12x approximations and the complex electronic structure of the –SNO group, it is important to first benchmark the CCSD(T)-F12 calculations against conventional CCSD(T)/CBS data. Once verified and calibrated, F12x coupled-cluster calculations using triple- or even double-zeta quality basis sets can be used to accurately assess the acid-base properties of HSNO (and potentially other small model RSNOs) in the gas phase. These high-level reference data in turn can be used to benchmark modern DFT model chemistries that will allow, in conjunction with polarizable continuum and hybrid QM/MM methods, accurate modeling of the reactivity of larger RSNOs in solution and/or protein environment.

Thus, the goal of this work is several-fold: first, we assess the performance of the explicitly-correlated CCSD(T)-F12x calculations against the previously reported conventional CCSD(T)/CBS reference data on HSNO, as well as investigate the possibility of estimating the effect of quadruple excitations in coupled cluster expansion using small double-zeta basis sets. We further use the CCSD(T)-F12x methods to evaluate the anharmonic vibrational frequencies for HSNO and investigate its gas-phase acid-base properties by calculating protonated and deprotonated forms of HSNO, with emphasis not only on the energetic effects, but also on the modification of the S–N bond properties. Finally, we evaluate the performance of a variety of modern DFT functional/basis set combinations against the reference coupled-cluster data.

Computational Details

Ab initio electronic structure calculations were performed using Molpro 2012.1 program package (Werner et al., 2012) and MRCC code (K´allay) interfaced with CFOUR 1.0 (Stanton et al., 2009). Molecular geometry optimization was conducted with frozen-core conventional (Hampel, Peterson, & Werner, 1992; Raghavachari, Trucks, Pople, & Head-Gordon, 1989) and explicitly correlated F12x (x = a, b, c) (Adler et al., 2007; Knizia et al., 2009) coupled cluster methods with single and double excitations CCSD (CCSD-F12a, CCSD-F12b, CCSD-F12c respectively) using the default optimization procedure and convergence criteria for stationary points and transition states implemented in Molpro 2012.1. These results were further improved with including the unscaled perturbative triple excitations (CCSD(T), CCSD(T)-F12a, CCSD(T)-F12b, CCSD(T)-F12c) or scaled triple excitations CCSD(T_{sc})-F12c as implemented in Molpro 2012.1. Perturbative quadruple excitations CCSDT(Q) were calculated using MRCC code interfaced with CFOUR program.

Considering significant computational cost of CCSDT(Q) calculations, the geometry optimizations with numerical gradients were performed using DL-FIND (Kästner et al., 2009) code using in-house interface with CFOUR to split the tasks across multiple nodes of a computational cluster as described in (Ivanova et al., 2014). Stationary points with CCSDT(Q) were optimized using the L-BFGS (Liu & Nocedal, 1989; Nocedal 1980) method in Cartesian coordinates and transition states were found with the partitioned rational functional optimization (P-RFO) (Baker 1986; Banerjee, Adams, Simons, & Shepard, 1985; Cerjan & Miller, 1981; Simons, Joergensen, Taylor, & Ozment, 1983)

using delocalized internal coordinates (DLC) with total connections (TC) (Billeter, Turner, & Thiel, 2000). The convergence criteria were 4.5×10^{-5} au and 1.0×10^{-6} au for the component of gradient and energy change, respectively.

Harmonic vibrational frequencies and zero-point vibrational energies (ZPEs) were calculated numerically at all levels of theory except CCSDT(Q). No scaling factor was applied to the vibrational mode values. Automated calculations of anharmonic vibrational frequencies and zero-point energies using VSCF and VCI methods in Molpro 2012.1 are performed as described in (Hrenar, Werner, & Rauhut, 2007; Neff & Rauhut, 2009; Rauhut 2004; Rauhut & Hrenar, 2008). Values of the standard T1 and D1 diagnostics (Janssen & Nielsen, 1998; Lee & Taylor, 1989) were used to estimate the quality of single-reference description of the corresponding wavefunction.

The basis sets used for geometry optimization in combination with explicitly correlated F12x coupled cluster method included augmented correlation consistent basis sets by Dunning, aug-cc-pVnZ (n = D, T, Q) (Kendall, Dunning, & Harrison, 1992) for all elements except sulfur, for which the correlation-consistent basis sets augmented with additional tight d-functions aug-cc-pV(n+d)Z were employed (Dunning Jr, Peterson, & Wilson, 2001) (will be referred to in text as AVnZ, n = D, T, Q). Also, optimized for explicitly correlated methods F12 basis sets of Peterson et al. cc-pVnZ-F12 (n = D, T, Q) (Peterson, Adler, & Werner, 2008), were used (will be referred to as VnZ-F12, n = D, T, Q). For explicitly correlated coupled cluster calculations with VnZ-F12 basis sets, the corresponding VnZ-F12/OPTRI basis sets are used by default to construct the complementary auxiliary orbital basis (CABS). For other orbital basis sets, appropriate JKFIT sets are used as the default setting in Molpro 2012.1.

To study the effect of perturbative triple and quadruple excitations, the difference between the frozen-core CCSD(T) and CCSD results, or CCSDT(Q) and CCSD(T) results, was calculated. In addition to aug-cc-pV(n+d)Z and cc-pVnZ-F12 basis sets, the effect of perturbative triples was explored with smaller basis sets, including Huzinaga's MIDI (*Gaussian Basis Sets for Molecular Calculations* 1984) and MIDI! (Easton, Giesen, Welch, Cramer, & Truhlar, 1996), 3-21G (Binkley, Pople, & Hehre, 1980; Gordon, Binkley, Pople, Pietro, & Hehre, 1982) , 6-31G, 6-31+G(d), 6-31G** and 6-31++G** (Francl et al., 1982; Hehre, Ditchfield, & Pople, 2003), pVDZ (Schäfer, Horn, & Ahlrichs, 1992) as well as the correlation-consistent 'seasonal' ladder of the basis set augmentation with diffuse functions proposed by Thrular (Papajak & Truhlar, 2010; Papajak, Zheng, Xu, Leverentz, & Truhlar, 2011): aug-cc-pV(D+d)Z, jul-cc-pV(D+d)Z, jun-cc-pV(D+d)Z, cc-pV(D+d)Z. The effect of perturbative quadruples was calculated using MIDI!, cc-pV(D+d)Z and jun-cc-pV(D+d)Z basis sets (Feller 1996; Schuchardt et al., 2007).

Density functional theory calculations were performed with Gaussian 09 Rev. D01 program package (Frisch et al., 2009) with 'UltraFine' integration grid (99 radial shells, 590 angular points per shell). Also, QChem 4.2 code (Krylov & Gill, 2013; Shao et al., 2006) was used to test the performance of selected DFT functionals. Used basis sets include double-ζ and triple-ζ quality def2-SV(P) and def2-TZVPPD by Weigend and Ahlrichs (Weigend & Ahlrichs, 2005) with diffuse functions by Rappoport and Furche (Rappoport & Furche, 2010), and segmented contracted aug-pcseg-1 and aug-pcseg-2 basis sets by F. Jensen (Jensen 2014). The def2-SV(P) basis set was further augmented by a tight d function at the sulfur atom with $\zeta = 2.994$ (Wang & Wilson, 2005) and the re-

sulting basis set is denoted as def2-SV(P)+d. In total, 45 DFT fucntionals are tested in this work (Table S1 in Supporting Information).

I. Improved *Ab Initio* Treatment of the S–N Bond Properties in HSNO

As mentioned in (Hochlaf et al., 2013; Ivanova et al., 2014; Timerghazin et al., 2008), potential energy surface of the singlet ground-state (X^1 A') HSNO contains two global minima (*cis*-HSNO and *trans*-HSNO conformations, respectively), connected by the transition state (Figure 1). Some of the biologically relevant isomerization pathways of HSNO molecule were thoroughly studied in (Ivanova et al., 2014), whereas the present study is focused only on the HSNO conformations and the protonated/deprotonated forms of *trans*-HSNO.

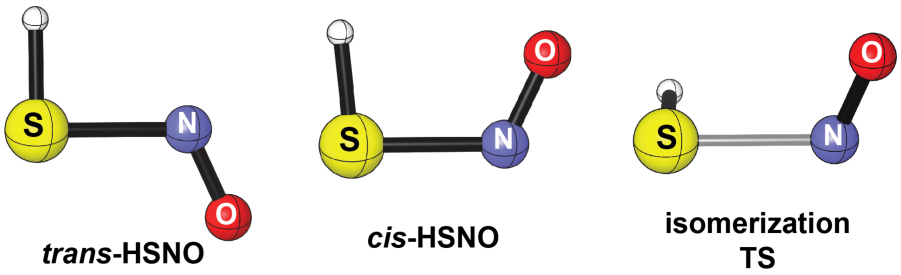

Figure 1. HSNO conformers and the transition state of their interconversion.

Table 1 summarizes the S–N bond lengths and relative energy of *trans*-HSNO and *cis*-HSNO, as well as the homolytic S–N bond dissociation energy in *trans*-HSNO. Table 2 summarizes geometric properties and activation energy of the transition state of inter-conversion reaction between *cis*-HSNO and *trans*-HSNO. Remaining geometric parameters for the HSNO conformers are presented in Tables S2-S4 in Supporting Information.

Table 1. Geometric and energetic properties of *trans*-HSNO and *cis*-HSNO.

Method	Basis set	*trans*-HSNO		*cis*-HSNO	ΔE(*trans-cis*), kcal/mol	
		r(S–N), Å	D_0(S–N), kcal/mol	r(S–N), Å	EE	EE + ZPE
CCSD(T)	CBS	1.837**	31.72*	1.821**	-0.90**	-0.80**
CCSD(T)-F12a	aug-cc-pV(D+d)Z	1.838	32.69	1.821	-0.91	-0.75
	aug-cc-pV(T+d)Z	1.839	31.55	1.821	-0.91	-0.77
	aug-cc-pV(Q+d)Z	1.838	31.47	1.820	-0.91	-0.78
	VDZ-F12	1.838	32.01	1.820	-0.92	-0.78
	VTZ-F12	1.839	31.42	1.821	-0.91	-0.77
	VQZ-F12	1.838	31.42	1.820	-0.90	-0.77
CCSD(T)-F12b	aug-cc-pV(D+d)Z	1.836	32.15	1.820	-0.92	-0.76
	aug-cc-pV(T+d)Z	1.838	31.33	1.820	-0.92	-0.78
	aug-cc-pV(Q+d)Z	1.838	31.34	1.820	-0.91	-0.78
	VDZ-F12	1.836	31.65	1.819	-0.93	-0.78
	VTZ-F12	1.838	31.21	1.820	-0.92	-0.78
	VQZ-F12	1.837	31.30	1.820	-0.90	-0.76
CCSD(T)-F12c	aug-cc-pV(D+d)Z	1.827	-	1.810	-0.89	-0.74
	aug-cc-pV(T+d)Z	1.832		1.816	-0.89	-0.76
	aug-cc-pV(Q+d)Z	1.835		1.818	-0.90	-0.78
	VDZ-F12	1.830		1.812	-0.90	-0.76
	VTZ-F12	1.833		1.818	-0.90	-0.77
	VQZ-F12	1.835		1.819	-0.90	-0.77
CCSD(T_{sc})-F12c	aug-cc-pV(D+d)Z	1.834	-	1.818	-0.90	-0.75
	aug-cc-pV(T+d)Z	1.835		1.819	-0.90	-0.76
	aug-cc-pV(Q+d)Z	1.836		1.819	-0.90	-0.78
	VDZ-F12	1.836		1.819	-0.91	-0.77
	VTZ-F12	1.836		1.819	-0.91	-0.77
	VQZ-F12	1.837		1.820	-0.90	-0.77

* (Timerghazin et al., 2008)

** (Ivanova et al., 2014)

Table 2. Geometric and energetic properties of the TS of cis-trans HSNO isomerization.

Method	Basis set	*r*(S–N), Å	∠O-N-S-H,°	$\Delta E^{\neq}$ (EE), kcal/mol	$\Delta E^{\neq}$ (EE + ZPE), kcal/mol
CCSD(T)	CBS	2.012*	87.51*	8.99*	8.16*
CCSD(T)-F12a	aug-cc-pV(D+d)Z	2.005	87.57	9.14	8.29
	aug-cc-pV(T+d)Z	2.012	87.53	9.02	8.18
	aug-cc-pV(Q+d)Z	2.012	87.51	9.01	8.16
	VDZ-F12	2.009	87.73	9.14	8.29
	VTZ-F12	2.013	87.60	8.99	8.14
	VQZ-F12	2.012	87.55	8.99	8.15
CCSD(T)-F12b	aug-cc-pV(D+d)Z	2.007	87.53	9.20	8.34
	aug-cc-pV(T+d)Z	2.013	87.51	9.05	8.20
	aug-cc-pV(Q+d)Z	2.011	87.50	9.03	8.19
	VDZ-F12	2.009	87.70	9.21	8.36
	VTZ-F12	2.012	87.58	9.02	8.18
	VQZ-F12	2.011	87.55	9.01	8.16
CCSD(T)-F12c	aug-cc-pV(D+d)Z	1.993	87.39	9.28	8.42
	aug-cc-pV(T+d)Z	2.006	87.46	9.09	8.24
	aug-cc-pV(Q+d)Z	2.088	87.48	9.04	8.21
	VDZ-F12	2.001	87.59	9.18	8.33
	VTZ-F12	2.007	87.53	9.03	8.20
	VQZ-F12	2.009	87.52	9.01	8.18
CCSD(T_{sc})-F12c	aug-cc-pV(D+d)Z	2.008	87.50	9.28	8.43
	aug-cc-pV(T+d)Z	2.011	87.49	9.08	8.23
	aug-cc-pV(Q+d)Z	2.011	87.49	9.03	8.20
	VDZ-F12	2.012	87.67	9.18	8.33
	VTZ-F12	2.012	87.56	9.02	8.18
	VQZ-F12	2.011	87.54	9.00	8.16

* (Ivanova et al., 2014)

According to the data in Tables 1, 2, S2-S4, and previously published results (Ivanova et al., 2014; Timerghazin et al., 2008), S–N bond properties that define the unusual behavior of the SNO group, are the most difficult to reproduce quantitatively even using the high-level *ab initio* methods. For instance, the S–N bond length in *trans*-HSNO is significantly overestimated with small basis sets (double-ζ and triple-ζ quality) at the CCSD(T) level of theory (1.903 Å with AVDZ basis set (Timerghazin et al., 2008) versus 1.837 Å after the CBS extrapolation (Ivanova et al., 2014)). The strong dependence of the performance of coupled cluster methods on the single-electron basis set size is well known (Timerghazin et al., 2008) and can be illustrated by the fact that the CBS limit of

the S–N bond length is approached only with the 5-ζ quality basis set (1.841 Å, Figure 2) (Ivanova et al., 2014). Such calculations are possible at the present moment only for the smallest S–nitrosothiols, namely isomers of HSNO, and quickly become prohibitively expensive with increasing size of the molecule.

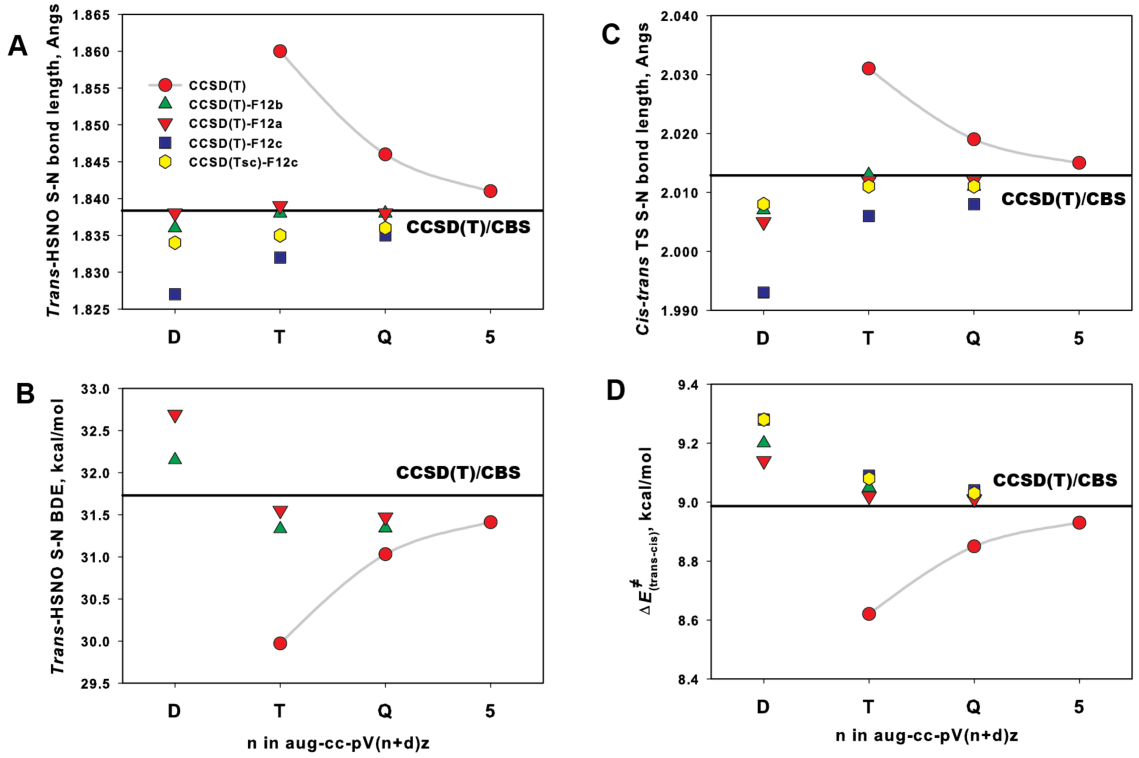

Figure 2. Dependence of geometric and energetic properties of the HSNO isomers on the basis set size for traditional and explicitly correlated coupled cluster method.

Similar trend is observed for the S–N bond length in slightly less stable *cis*-HSNO: the CBS limit 1.821 Å, calculated in (Ivanova et al., 2014), is, by far, the best represented with AV5Z basis set (1.825 Å) and significantly overestimated with AVDZ basis set (1.894 Å). The other geometric parameters (N-O, H-S bond lengths, valence angles) converge noticeably faster to the CBS limit, and, therefore, are not limiting the overall performance of the given method. Relative instability of *cis*-HSNO in comparison

to *trans*-HSNO is less sensitive to the basis set deficiency. Plausibly, the mutual error cancellation occurs: the CCSD(T)/CBS limit 0.90 kcal/mol is reproduced reasonably well even with the smallest in the series AVDZ basis set (0.97 kcal/mol) (Ivanova et al., 2014).

The homolytic S–N bond dissociation energy in trans-HSNO is, in opposite, highly underestimated with small basis sets (CCSD(T)/CBS limit is 31.72 kcal/mol accounting the electronic energy only, CCSD(T)/AVDZ value is 27.74 kcal/mol, CCSD(T)/AV5Z value is 31.41 kcal/mol). The S–N bond in the transition state is even more elongated in comparison to *trans*-HSNO and *cis*-HSNO: the CBS extrapolation at CCSD(T) level predicts the value of 2.012 Å, CCSD(T)/AVDZ and CCSD(T)/AV5Z simulations predict 2.067 Å and 2.015 Å, respectively. Activation barrier of the isomerization reaction tends to be noticeably underestimated at the CCSD(T) level of theory, with the CCSD(T)/CBS limit at 8.99 kcal/mol and CCSD(T)/AVDZ result of 8.08 kcal/mol.

Based on these observations, the first problem with applying the coupled cluster methodology to calculate the properties of HSNO molecule is immediately apparent. It stems from the strong dependence of the abovementioned properties on the single electron basis set size, requiring using at least the 5-ζ quality basis sets for all calculations. Recently, the explicitly correlated coupled cluster methods F12x (F12a, F12b, F12c) were proposed to mitigate this issue and extend their potential applicability towards larger chemical systems.

II. Performance of Explicitly Correlated Coupled Cluster Methods

In this work, we perform an assessment of the performance of explicitly correlated coupled cluster methods F12x (F12a, F12b, F12c) in comparison to conventional coupled cluster method with CBS extrapolation (Ivanova et al., 2014; Timerghazin et al., 2008). Figure 2 illustrates the performance changes for the S–N bond lengths in trans-HSNO and the transition state, S–N BDE and the activation barrier for *cis-trans* isomerization reaction.

Implementation of the terms, explicitly accounting for the interelectronic distances, to the coupled cluster theory (Adler et al., 2007; Knizia et al., 2009), has shown to have an incredible effect on the basis set convergence: it was recently referred to in the literature as "two zeta gain rule", e.g. 5-ζ quality results are often obtained with the 3-ζ basis sets (Martin & Kesharwani, 2014).

To ensure the reliability and reproducibility of the explicitly correlated coupled cluster theory results in our work, the typical coupled cluster diagnostic values for non-dynamic electron correlation for the *cis*-HSNO, *trans*-HSNO and the TS (T1, D1, and the largest T2 amplitudes) were collected (Tables S5 in Supporting Information). In case of *trans*-HSNO, the T1 and D1 diagnostic values (0.024…0.027 and 0.071…0.078, respectively) obtained with CCSD(T)-F12x methods are almost identical to the ones obtained with conventional coupled cluster method CCSD(T) (0.027 and 0.076) in (Timerghazin et al., 2008). The values of the largest T2 amplitudes for trans-HSNO (0.060…0.092) are generally above the threshold value (0.050), which may indicate the non-negligible effect of the post-CCSD(T) effects in coupled cluster method. Diagnostic values for *cis*-HSNO

and the isomerization TS indicate very similar behavior of their electronic structure, which, therefore, requires identical computational treatment as in the case of trans-HSNO.

We found that the properties of HSNO conformers were affected by the implementation of the F12x theory by significant acceleration of the basis set convergence. For example, S–N bond lengths are often almost quantitatively represented even with the smallest double-ζ quality basis sets: CCSD(T)-F12a/aug-cc-pV(D+d)Z data are in excellent agreement with the CCSD(T)/CBS values, 1.838 Å for *trans*-HSNO (1.837 Å with CBS), 1.821 Å for *cis*-HSNO (1.821 Å with CBS), 2.005 Å for the TS (2.012 Å with CBS). Further increase of the angular momentum of the basis sets has almost no effect on the S–N bond lengths and the other geometric parameters (see SI Tables S2-S4). Therefore, for the geometries of HSNO conformers the "two zeta gain rule" almost turns into the remarkable "three zeta gain rule". CCSD(T)F12a and CCSD(T)F12b have the fastest convergence on the basis set size when applied to trans-HSNO S-N bond length, comparing to CCSD(T)F12c and CCSD(T_{sc})F12c. CCSD(T_{sc})F12c, on the other hand, converges faster for calculating the S-N bond length in isomerization TS.

The energetic properties, on the other hand, were found to require at least triple-ζ quality basis set to adequately match the performance of CCSD(T)/CBS approach. The S–N BDE in *trans*-HSNO show weaker sensitivity to the basis set with regard to the conventional coupled cluster method. Interestingly, S–N BDE is overestimated with the small basis sets using CCSD(T)-F12a theory, and converges to the CBS level from above. Thus, moving from the double-ζ to the triple-ζ quality basis set shifts the BDE value closer to the CBS limit (31.72 kcal/mol): 32.69 and 31.55 kcal/mol calculated with

CCSD(T)-F12a/aug-cc-pV(D+d)Z and CCSD(T)-F12a/aug-cc-pV(T+d)Z, respectively. Increase of the basis set to quadruple-ζ has only marginal effect on BDE values. Current implementation of CCSD(T)F12c and CCSD(T_{sc})F12c methods in Molpro 2012.1 (Werner et al., 2012) does not allow calculations of the species with open-shell electronic character, and, therefore, they cannot be used to obtain corresponding BDE values.

Activation barrier of the *cis-trans* isomerization reaction behaves similarly to the S–N BDE values when CCSD(T)-F12a method is applied, and also converges to the CBS level from above. Triple-ζ quality basis sets provide almost quantitative representation of the CCSD(T)/CBS barrier height (8.16 kcal/mol): 8.18 kcal/mol with CCSD(T)-F12a/aug-cc-pV(T+d)Z, 8.29 kcal/mol with CCSD(T)-F12b/aug-cc-pV(D+d)Z. CCSD(T)F12c and CCSD(Tsc)F12c tend to converge slower on the basis set size.

At the first look, the present study does not reveal a significant advantage of any particular implementation of explicitly correlated coupled cluster theory over the other (F12a, F12b or F12c), although the previous data (Martin & Kesharwani, 2014) show that the CCSD(T)-F12a method performs better for energetic quantities when small (double-ζ or triple-ζ) basis sets are used. Also, systematic difference in performance between two series of the basis sets, aug-cc-pV(n+d)Z] and VnZ-F12, is not immediately clear. To compare the performance of each particular combination of the F12x method and the basis set, we used the sum of unsigned relative deviations from the CCSD(T)/CBS values (*S*, %) as an indicator of performance (lower *S* value is better, as shown on Figure 3).

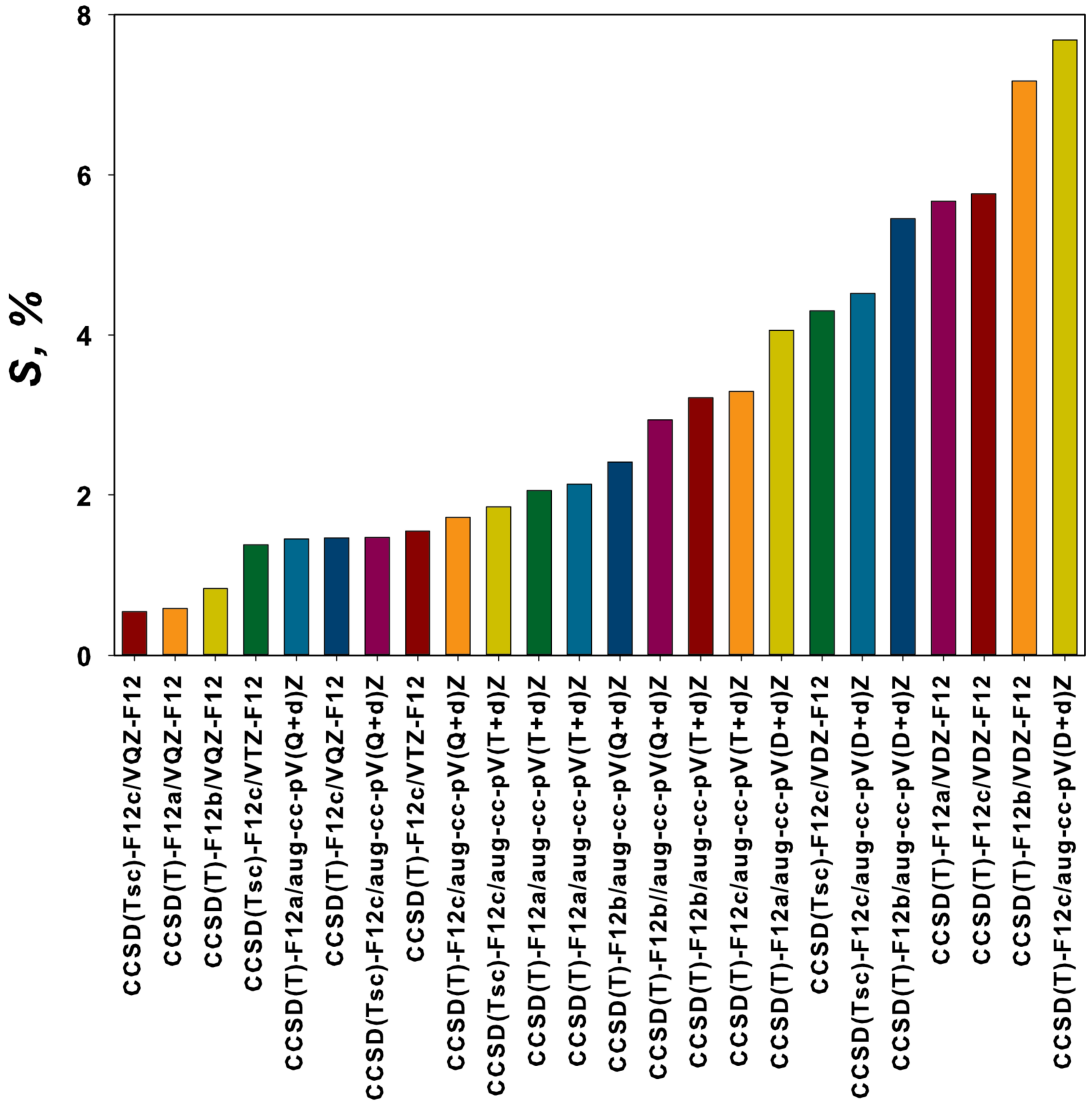

Figure 3. Relative performance of the explicitly correlated coupled cluster methods.

The best performance with regard to the CBS-extrapolated CCSD(T) values is achieved at CCSD(T_{sc})-F12c/VQZ-F12 level. That method will be used in this work when possible to generate reference data (except the cases with open-shell species, where the second best-performing combination, CCSD(T)-F12a/VQZ-F12, is used).

III. Accounting for the Quadruple Excitations in Coupled Cluster Method

Besides slow convergence of the RSNO properties on the basis set size, the S–N bond properties demonstrate very slow convergence with respect to the excitation level in coupled cluster treatment. An abrupt change of the S–N bond lengths and BDEs moving from the CCSD to the CCSD(T) method with the same basis set was described in (Timerghazin et al., 2008): CCSD systematically underestimates the S–N bond length in HSNO by ~0.04 Å, while the S–N BDE is underestimated by ~5 kcal/mol. Influence of the perturbative quadruple excitations was estimated using only relatively small basis set (Ahlrichs pVDZ) and restricted optimization procedure (only the S–N bond length was optimized) as ~0.02 Å for the S–N bond length in *trans*-HSNO (increase from the CCSD(T) value), and ~1 kcal/mol for the S–N BDE (increase from the CCSD(T) value).

Recent work of (Ivanova et al., 2014) provides an improved estimation of the Δ(Q) effect using larger cc-pVDZ basis set and non-constrained optimization of the HSNO geometry. In *trans*-HSNO, S–N bond length elongates from the CCSD/CBS value by 0.041 Å with inclusion of the perturbative triples and by 0.033 Å with perturbative quadruple excitations, the S–N BDE increases with Δ(T) by 5.66 kcal/mol, and with Δ(Q) by 1.30 kcal/mol. The activation barrier of the *cis-trans* interconversion reaction is increased by 0.54 kcal/mol by accounting for the (Q) excitations. Therefore, a conclusion can be drawn that performing calculations even at the CCSD(T)/CBS level of theory is not sufficient for quantitative representation of the HSNO properties and needs to be supplemented with an adequate yet inexpensive way of accounting for the effect of the quadruple excitations.

Promising observation was made in (Timerghazin et al., 2008): the contribution of perturbative triple excitations to the S–N bond lengths and dissociation energies is almost independent on the size of the used basis set. At the same time, current implementation of the explicitly correlated coupled cluster method CCSD(T)-F12x does not affect the procedure of perturbative triple excitations calculation, which is identical to traditional coupled cluster method (Martin & Kesharwani, 2014; Werner et al., 2012). The questions arise, would the effect of the triple excitations be conserved when a broader variety of the basis sets is used and would the quadruple excitations behave similarly?

In this work, we examine the dependence of the Δ(T) and Δ(Q) corrections using conventional coupled cluster method on the basis set. Table 3 contains the list of properties of HSNO isomers, calculated with CCSD, CCSD(T) and CCSDT(Q) methods with a variety of basis sets. Graphical representation of some of those data is also shown on Figure 4.

It is immediately apparent, that contribution of Δ(T) corrections in all cases exceed the contribution of Δ(Q) corrections. S–N bond length changes decay relatively slow with the increase of the excitation level of coupled cluster theory within the same basis set: in *trans*-HSNO, the elongation by 0.057 Å occurs when applying perturbative triples (with the cc-pV(D+d)Z basis set), and elongation by 0.033 Å when applying the perturbative quadruple excitations. In *cis*-HSNO, the values are 0.059 Å and 0.035 Å, respectively. These values are, as expected, in perfect agreement with the ones published previously (Ivanova et al., 2014), despite the fact that tight d-functions are used in the basis set employed in this work. The S–N bond length in TS, already stretched in regard to the *trans*-HSNO, converges faster with the coupled cluster theory expansion using cc-

pV(D+d)Z basis set. The trifold excess of Δ(T) over Δ(Q) (0.078 Å vs. 0.025 Å) indicates similarities of the transition state electronic structure in comparison to the stationary points.

Energetic parameters were found to be sensitive to the level of coupled cluster excitations too. As an example, the S–N BDE in *trans*-HSNO is underestimated by 4.82 kcal/mol when omitting perturbative triples, and by 1.42 kcal/mol when omitting perturbative quadruples (with the cc-pV(D+d)Z basis set). Relative instability of *cis*-HSNO versus *trans*-HSNO is, similarly, underestimated by 0.12 kcal/mol and 0.11 kcal/mol. Distinctly, the isomerization reaction barrier is changing in opposite directions after consecutive application of the Δ(T) and Δ(Q) corrections.

Overall, contribution of the perturbative triple exciations to the properties of HSNO conformations in the present study remains remarkably constant even with the use of broad selection of common basis sets. Calculating effects of the perturbative quadruple excitations is extremely expensive, and, therefore, it was limited only to the cc-pV(D+d)Z and MIDI! basis sets (to compare with the results obtained with cc-pVdZ in (Ivanova et al., 2014)). In all cases, we observe conclusive conservation of the trends when these three basis sets are used. Therefore, an additional accounting for the Δ(Q) corrections for the HSNO properties, even made with the small MIDI! basis set (when the cost of more rigorous description is prohibitively high), will still improve the quality of CCSD(T)-F12x calculations.

Table 3. Contribution of the post-CCSD corrections to the properties of HSNO isomers.

Method	Basis set	*trans*-HSNO		*cis*-HSNO	ΔE(*trans* - *cis*), kcal/mol	TS of HSNO isomer-izaion	
		r(S–N), Å	D_0(S–N), kcal/mol	*r*(S–N), Å		*r*(S–N), Å	*cis-trans* $\Delta E^{\neq}$ (EE), kcal/mol
CCSD	CBS	1.797*	26.06*	1.782*	-0.81*	-	-
	aug-cc-pV(D+d)Z	1.855	22.18	1.846	-0.99	1.997	8.24
	jul-cc-pV(D+d)Z	1.854	22.12	1.845	-1.03	2.048	9.97
	jun-cc-pV(D+d)Z	1.862	19.22	1.848	-1.04	2.008	8.14
	cc-pV(D+d)Z	1.891	18.26	1.874	-0.47	2.033	7.47
	pVDZ	1.859	17.67	1.839	-0.65	2.016	8.22
	6-31++G**	1.828	21.33	1.814	-0.94	1.971	9.19
	6-31G**	1.848	19.77	1.837	-0.85	1.992	8.53
	6-31+G(d)	1.827	21.38	1.811	-0.83	1.969	9.36
	6-31G	2.047	11.66	2.042	-1.29	2.212	6.22
	3-21G	2.045	15.15	2.038	-1.01	2.153	5.53
	MIDI!	1.924	23.55	1.915	-0.26	2.031	7.31
	MIDI	2.071	15.19	2.066	-0.93	2.137	6.21
Δ(T)	CBS	0.041*	5.66*	0.038*	-0.08*	-	-
	aug-cc-pV(D+d)Z	0.047	5.31	0.048	-0.06	0.070	-0.16
	jul-cc-pV(D+d)Z	0.046	5.28	0.047	-0.07	0.018	-1.72
	jun-cc-pV(D+d)Z	0.051	4.89	0.052	-0.12	0.078	-0.25
	cc-pV(D+d)Z	0.057	4.82	0.059	-0.12	0.078	-0.28
	pVDZ	0.055	4.54	0.054	-0.16	0.095	-0.44
	6-31++G**	0.038	4.46	0.036	-0.10	0.075	-0.14
	6-31G**	0.046	4.28	0.046	-0.09	0.080	-0.29
	6-31+G(d)	0.037	4.42	0.034	-0.11	0.076	-0.10
	6-31G	0.060	3.87	0.063	0.02	0.048	-0.71
	3-21G	0.066	3.77	0.068	0.03	0.098	-0.40
	MIDI!	0.042	4.72	0.042	-0.08	0.060	0.05
	MIDI	0.047	3.80	0.047	0.01	0.099	-0.87
Δ(Q)	cc-pV(D+d)z	0.033	1.42	0.035	0.11	0.025	0.50
	cc-pVDZ	0.033**	1.30**	0.034**	0.10**	0.025**	0.54**
	MIDI!	0.022	1.39	0.022	0.11	0.015	0.65
ΔCV	cc-pCVDZ-F12	-0.002	-0.28	-0.001	0.01	-0.002	-0.02
	cc-pCVTZ-F12	-0.005	-0.04	-0.005	0.01	-0.007	0.08

* (Timerghazin et al., 2008)
** (Ivanova et al., 2014)

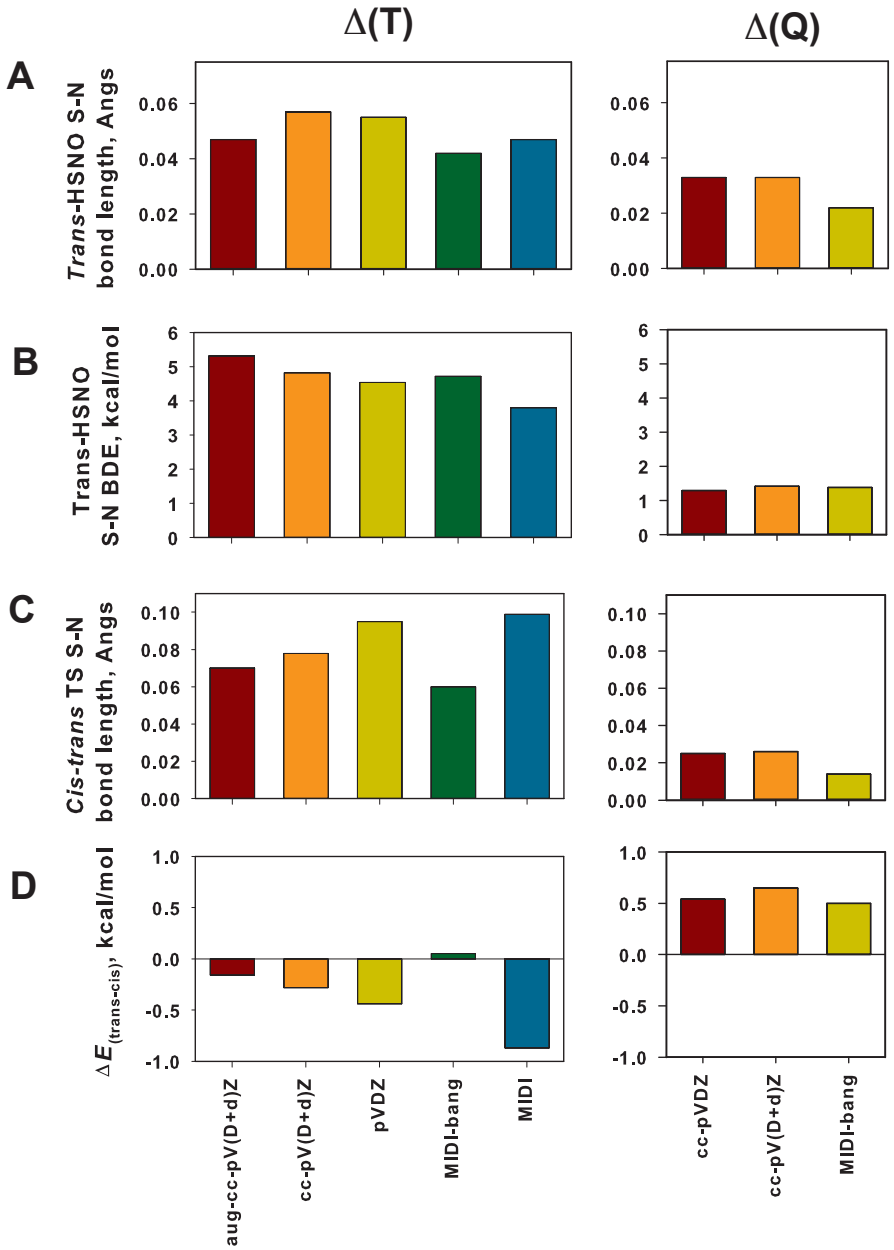

Figure 4. Contribution of the perturbative triple and quadruple excitations to the properties of HSNO isomers, calculated with different basis sets.

IV. Accounting for the Core-Valence Correlation

Another important post-HF effect, that arises when the frozen-core assumption is implied, is the influence of core-valence electron correlation. In particular cases, when high accuracy is needed to obtain molecular geometries (at sub-picometer level) and thermochemical parameters (within 1 kcal/mol uncertainty), this effect cannot be disregarded (Dixon, Feller, Peterson, Wheeler, & Tschumper, 2012; Peterson, Feller, & Dixon, 2012).

The problem with slow convergence of the correlation energies to the CBS limit when conventional coupled cluster method is used in combination with correlation-consistent family of the basis sets, as mentioned in (Hill, Mazumder, & Peterson, 2010), is similar to the slow convergence of the S–N bond properties mentioned above. One of the approaches to remedy this problem is to use the explicitly correlated coupled cluster methods, that allows one to achieve a reasonable converged results with the triple-ζ quality basis set, whereas the conventional CCSD(T) converge only at impractical 6-ζ level.

Recently, basis sets for calculating the core-valence correlation effects were developed to match the explicitly correlated *ab initio* methods (Hill, Mazumder, & Peterson, 2010). In this work, we provide the reference values of the HSNO properties, including best-of-our-knowledge CCSD(T) results (either with the CBS extrapolation, or as close as possibly matching the CBS level CCSD(T)-F12x data), as well as the contribu-

tions of the perturbative quadruple excitations Δ(Q) and core-valence correlation ΔCV (Table 9).

The ΔCV effect on the S–N bond lengths for *cis*-HSNO, *trans*-HSNO and the interconversion TS lies within the 0.005 Å margin, significantly lower than the corresponding values of the Δ(Q) corrections. The effect of core-valence correlation on the energetic parameters is similarly less pronounced, but still contributes to the overall quality of computational SNO group description.

V. Accounting for the Anharmonic Effect

Accurate calculations of the spectroscopic properties of HSNO conformations, as well as more accurate accounting of ZPE corrections, may require taking into consideration the anharmonicity of vibrational modes. Proposed in (Rauhut 2004) automatic procedure of generating multidimensional potential energy surfaces, as implemented in Molpro (Werner et al., 2012), was used in this work in combination with the vibrational self-consustent field (VSCF) or vibrational configuration interaction (VCI) methods to calculate the anharmonic vibrational modes for *cis*-HSNO and *trans*-HSNO (Table 4). Harmonic vibrational frequencies, calculated within CCSD(T)-F12a/aug-cc-pV(Q+d)z approximation, are also listed for comparison in Table 4 along with the experimental data from (Nonella, Huber, & Ha, 1987).

As immediately apparent from the data in Table 4, one of the most characteristic vibration modes of the HSNO molecule – S–N bond stretch – depends significantly on the level of theoretical treatment. Harmonic CCSD(T)-F12a/aug-cc-pV(Q+d)z values are

in somewhat good agreement with the anharmonic VCISDTQ values obtained with a much smaller double-ζ basis set (324.6 and 325.1 cm^{-1} for *trans*-HSNO, 346.1 and 342.5 cm^{-1} for *cis*-HSNO), and differ from the experimental data (386.5 cm^{-1} for *trans*-HSNO, 406.5 cm^{-1} for *cis*-HSNO). The direct comparison of the calculated values representing gaseous phase, and experimental data obtained at low temperatures in argon matrices, should not be used to assess the performance of a given computational method, but rather to help making a correct assignment of the individual vibrations. In this sense, the experimental data agree reasonably with our theoretical simulations.

Table 4. Harmonic and anharmonic vibrational modes (cm^{-1}) of *cis*-HSNO and *trans*-HSNO, and corresponding ZPE (kcal/mol) values

Mode	Experiment (Nonella, 1987)		CCSD(T)-F12a/aug-cc-pV(D+d)z				CCSD(T)-F12a/aug-cc-pV(Q+d)z		Recommended values	
			Harmonic		Anharmonic correction		*Trans*	*Cis*	*Trans*	*Cis*
	Trans	*Cis*	*Trans*	*Cis*	*Trans*	*Cis*				
1 A`/S–N stretching	297.0	307.0	331.2	352.4	-6.1	-9.9	324.6	346.1	318.5	336.1
2 A``/H-S–N-O bending	386.5	406.5	396.5	425.5	-15.7	-19.6	392.4	427.4	376.8	407.7
3 A`/S–N-O scissoring	543.5	503.0	583.1	532.3	-18.1	-10.3	577.5	530.3	559.4	520.0
4 A`/H-S–N bending	877.5	858.5	929.7	907.5	-29.8	-20.3	925.6	906.1	895.8	885.8
5 A`/N-O stretching	1596.0	1570.0	1622.4	1599.9	-23.5	-19.9	1622.9	1599.5	1599.5	1579.6
6 A`/S-H stretching	2613.0	2566.0	2723.7	2666.8	-108.9	-110.4	2721.5	2665.9	2612.6	2555.5
ZPE	9.03	8.88	9.42	9.27	-	-	9.38	9.26	9.10	8.98

Table 5a. Harmonic and anharmonic vibrational modes (cm^{-1}) of N-protonated *trans*-HSNO, and corresponding ZPE (kcal/mol) values.

Mode	CCSD(T)-F12a/aug-cc-pV(D+d)z		CCSD(T)-F12a/aug-cc-pV(Q+d)z	Recommended values
	Harmonic	Anharmonic correction		
1 A``	450.8	-13.3	454.45	441.2
2 A`	452.4	-4.8	456.11	451.3
3 A`	785.5	-20.2	787.67	767.5
4 A``	901.9	-19.6	911.49	891.9
5 A`	1056.7	-26.5	1052.42	1026.0
6 A`	1495.7	-42.8	1496.71	1453.9
7 A`	1590.63	-23.0	1593.91	1570.9
8 A`	2659.83	-115.0	2654.34	2539.3
9 A`	3248.55	-154.7	3254.76	3100.1
ZPE	18.07	-	18.10	17.50

Table 5b. Harmonic and anharmonic vibrational modes (cm^{-1}) of O-protonated *trans*-HSNO, and corresponding ZPE (kcal/mol) values.

Mode	CCSD(T)-F12a/aug-cc-pV(D+d)z		CCSD(T)-F12a/aug-cc-pV(Q+d)z	Recommended values
	Harmonic	Anharmonic correction		
1 A`	448.2	-7.2	452.22	445.0
2 A``	594.0	-20.2	595.57	575.4
3 A``	708.5	-20.4	714.48	694.1
4 A`	878.2	-20.7	880.18	859.5
5 A`	1030.9	-27.1	1030.45	1003.3
6 A`	1255.1	-40.5	1257.79	1217.3
7 A`	1467.87	-42.5	1477.0	1434.5
8 A`	2650.49	-118.4	2647.85	2529.4
9 A`	3618.24	-189.4	3626.16	3436.7
ZPE	18.09	-	18.13	17.43

Table 5c. Harmonic and anharmonic vibrational modes (cm^{-1}) of S-protonated *trans*-HSNO, and corresponding ZPE (kcal/mol) values.

Mode	CCSD(T)-F12a/aug-cc-pV(D+d)z		CCSD(T)-F12a/aug-cc-pV(Q+d)z	Recommended values
	Harmonic	Anharmonic correction		
1	54.7	50.7	28.19	78.9
2	208.7	-2.8	204.91	202.1
3	335.8	6.4	331.18	337.6
4	463.3	-6.9	453.07	446.2
5	551.1	-24.7	544.99	520.3
6	1194.7	-12.2	1194.32	1182.1
7	2048.88	-21.7	2058.71	2037.0
8	2670.7	-135.2	2667.8	2532.6
9	2684.97	-134.3	2681.68	2547.4
ZPE	14.60	-	14.53	14.13

Table 5d. Harmonic and anharmonic vibrational modes (cm^{-1}) of deprotonated *trans*-HSNO, and corresponding ZPE (kcal/mol) values.

Mode	CCSD(T)-F12a/aug-cc-pV(D+d)z		CCSD(T)-F12a/aug-cc-pV(Q+d)z	Recommended values
	Harmonic	Anharmonic correction		
1 A`	491.0	-5.6	494.32	488.8
2 A`	735.1	-8.6	740.57	732.0
3 A`	1358.3	-28.0	1363.37	1335.3
ZPE	3.69	-	3.71	3.65

Table 6. Harmonic and anharmonic ZPE contributions (kcal/mol) to the energetic parameters of *trans*-HSNO.

Method	Basis set	HSNO D_0(S–N)	*cis-trans* $\Delta E^{\neq}$	ΔE (*trans-cis*)	N-prot. HSNO		O-prot. HSNO		S-prot. HSNO		Deprot. SNO	
					ΔE(H^+ transf.)	D_0(S–N)	ΔE(H^+ transf.)	D_0(S–N)	ΔE(H^+ transf.)	D_0(S–N)	ΔE(H^+ transf.)	D_0(S–N)
CCSD(T)-F12a harmonic	aug-cc-pV(Q+d)Z	-2.79	-0.85	0.13	0.34	-5.67	0.37	-5.78	-3.27	-1.55	2.71	-0.98
	VQZ-F12	-2.79	-0.84	0.13	0.31	-5.64	0.36	-5.78	-3.27	-1.55	2.71	-0.98
CCSD(T)-F12b harmonic	aug-cc-pV(Q+d)Z	-2.79	-0.84	0.13	0.34	-5.68	0.37	-5.77	-3.27	-1.55	2.71	-0.98
	VQZ-F12	-2.79	-0.84	0.14	0.31	-5.65	0.36	-5.77	-3.28	-1.54	2.71	-0.99
CCSD(T)-F12c harmonic	aug-cc-pV(Q+d)Z	-	-0.83	0.13	0.32	-	0.36	-	-3.28	-1.55	2.72	-
	VQZ-F12	-	-0.83	0.12	0.31	-	0.37	-	-3.27	-1.55	2.71	-
$CCSD(T_{sc})$-F12c harmonic	aug-cc-pV(Q+d)Z	-	-0.83	0.12	0.34	-	0.38	-	-3.26	-1.55	2.72	-
	VQZ-F12	-	-0.83	0.13	0.32	-	0.37	-	-3.26	-1.55	2.72	-
CCSD(T)-F12a anharmonic	aug-cc-pV(Q+d)Z/ aug-cc-pV(D+d)Z	-2.50	-	0.11	0.03	-5.07	-0.04	-5.08	-3.34	-1.19	2.94	-0.92

The ZPE values, calculated using different methods, remarkably, show that harmonic treatment can introduce additional errors to accurate thermochemical data for the HSNO isomers. Thus, the ZPE for trans-HSNO in harmonic approximation at the CCSD(T)-F12a/aug-cc-pV(Q+d)z level of theory is 0.25 kcal/mol higher than the anharmonic value obtained with the most computationally rigorous method (VCISDTQ, CCSD(T)-F12a/aug-cc-pV(D+d)z), and 0.26 kcal/mol higher in case of *cis*-HSNO. At the same time, within harmonic approximation and CCSD(T)-F12a level of theory, the ZPE values are almost converged with the increase of the basis set from double to quadruple-ζ (9.42 kcal/mol vs. 9.38 kcal mol for trans-HSNO, 9.27 kcal/mol vs. 9.26 kcal/mol for cis-HSNO). Therefore, when possible, the anharmonicity of vibrations should be taken into account for calculation of the properties of HSNO molecule.

VI. Acid-Base Properties of HSNO Molecule

In recent work of Filipovic (Filipovic et al., 2012), a strong peak at m/z 63.9898 corresponding to [HSNO + H+] species was observed on mass spectrum of acidified nitrite after neutralization with the potassium phosphate buffer at pH = 7.4. The nature of protonated species and relative basicity of an S, N and O atoms in HSNO molecule, although, remains unclear. Acidic properties of HSNO are also obscure. In (Quiroga, Almaraz, Amorebieta, Perissinotti, & Olabe, 2011), the pKa value of an iron-coordinated HSNO was estimated as high as 10.5, possibly indicating that the HSNO molecule at physiological pH should be mostly non-dissociated.

In this work, we perform a study of the acid-base properties of HSNO molecule using modified theoretical approach discussed above. The protonation/deprotonation reactions, assisted by a water molecule, are shown on Figure 5, as well as the energetic and geometric changes associated with these processes.

Tables 7 and 8 summarize the properties of protonated and deprotonated trans-HSNO molecule: S–N bond lengths, S–N BDEs and energy of the water-assisted proton transfer. Tables S6 and S7 in Supporting Information provide the coupled cluster diagnostic values for protonated/deprotonated forms of HSNO.

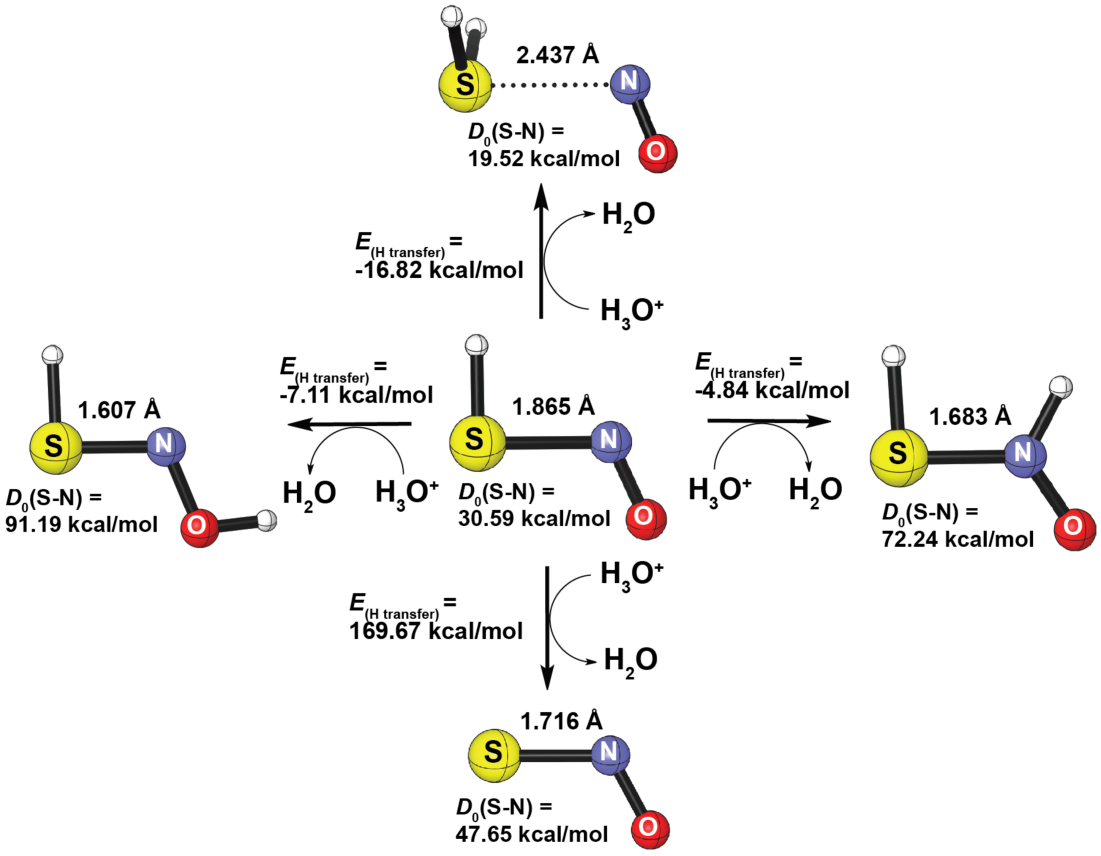

Figure 5. Reference values for the acid-base properties of trans-HSNO molecule (EE + Δ(Q) + ΔCV + ΔZPE_{anharm}).

Table 7a. Properties of N- and O-protonated trans-HSNO.

Method	Basis set	N-protonated trans-HSNO			O-protonated trans-HSNO		
		r(S–N), Å	D_0(S–N), kcal/mol	ΔE(H^+ transfer), kcal/mol	r(S–N), Å	D_0(S–N), kcal/mol	ΔE(H^+ transfer), kcal/mol
CCSD(T)-F12a	aug-cc-pV(D+d)Z	1.683	77.81	-5.07	1.606	96.66	-8.09
	aug-cc-pV(T+d)Z	1.681	76.52	-5.15	1.607	95.54	-7.93
	aug-cc-pV(Q+d)Z	1.681	76.37	-5.04	1.606	95.46	-7.82
	VDZ-F12	1.681	77.22	-5.61	1.607	96.35	-8.56
	VTZ-F12	1.681	76.40	-5.23	1.607	95.50	-8.23
	VQZ-F12	1.680	76.34	-5.08	1.606	95.45	-7.89
CCSD(T)-F12b	aug-cc-pV(D+d)Z	1.681	77.47	-5.50	1.606	96.32	-8.41
	aug-cc-pV(T+d)Z	1.681	76.39	-5.25	1.607	95.37	-7.99
	aug-cc-pV(Q+d)Z	1.680	76.30	-5.14	1.606	95.37	-7.89
	VDZ-F12	1.681	76.97	-5.74	1.607	96.08	-8.58
	VTZ-F12	1.681	76.27	-5.31	1.607	95.34	-8.06
	VQZ-F12	1.680	76.27	-5.15	1.606	95.37	-7.94
CCSD(T)-F12c	aug-cc-pV(D+d)Z	1.679	-	-5.50	1.603	-	-8.55
	aug-cc-pV(T+d)Z	1.679		-5.27	1.605		-8.08
	aug-cc-pV(Q+d)Z	1.680		-5.17	1.606		-7.97
	VDZ-F12	1.678		-5.60	1.604		-8.60
	VTZ-F12	1.679		-5.30	1.606		-8.13
	VQZ-F12	1.679		-5.17	1.605		-8.00
CCSD(T_{sc})-F12c	aug-cc-pV(D+d)Z	1.679	-	-5.45	1.606	-	-8.57
	aug-cc-pV(T+d)Z	1.679		-5.20	1.606		-8.04
	aug-cc-pV(Q+d)Z	1.680		-5.12	1.606		-7.93
	VDZ-F12	1.678		-5.53	1.607		-8.59
	VTZ-F12	1.679		-5.26	1.606		-8.11
	VQZ-F12	1.679		-5.14	1.606		-7.98

Table 7b. Properties of S-protonated and deprotonated trans-HSNO.

Method	Basis set	S-protonated *trans*-HSNO			Deprotonated *trans*-HSNO		
		r(S–N), Å	D_0(S–N), kcal/mol	ΔE(H^+ transfer), kcal/mol	*r*(S–N), Å	D_0(S–N), kcal/mol	ΔE(H^+ transfer), kcal/mol
CCSD(T)-F12a	aug-cc-pV(D+d)Z	2.437	20.69	-14.36	1.708	48.69	166.91
	aug-cc-pV(T+d)Z	2.445	20.28	-14.15	1.707	47.21	166.22
	aug-cc-pV(Q+d)Z	2.446	20.19	-14.17	1.706	46.97	165.98
	VDZ-F12	2.443	20.26	-15.28	1.705	48.59	168.01
	VTZ-F12	2.446	20.21	-14.52	1.706	47.69	166.76
	VQZ-F12	2.447	20.15	-14.36	1.705	47.33	166.30
CCSD(T)-F12b	aug-cc-pV(D+d)Z	2.441	20.58	-14.65	1.706	48.12	166.84
	aug-cc-pV(T+d)Z	2.446	20.25	-14.34	1.706	46.98	166.36
	aug-cc-pV(Q+d)Z	2.447	20.17	-14.30	1.706	46.85	166.14
	VDZ-F12	2.445	20.17	-15.43	1.704	48.18	168.00
	VTZ-F12	2.447	20.16	-14.62	1.705	47.47	166.84
	VQZ-F12	2.447	20.14	-14.45	1.705	47.23	166.42
CCSD(T)-F12c	aug-cc-pV(D+d)Z	2.451	20.21	-14.54	1.701	-	166.54
	aug-cc-pV(T+d)Z	2.450	20.08	-14.33	1.703		166.19
	aug-cc-pV(Q+d)Z	2.449	20.07	-14.38	1.704		166.16
	VDZ-F12	2.453	19.89	-15.44	1.700		167.61
	VTZ-F12	2.450	20.00	-14.70	1.703		166.77
	VQZ-F12	2.449	20.05	-14.52	1.703		166.45
CCSD(T_{sc})-F12c	aug-cc-pV(D+d)Z	2.433	21.06	-14.27	1.703	-	166.34
	aug-cc-pV(T+d)Z	2.443	20.37	-14.18	1.704		166.05
	aug-cc-pV(Q+d)Z	2.446	18.67	-14.30	1.704		166.08
	VDZ-F12	2.439	20.63	-15.20	1.702		167.45
	VTZ-F12	2.445	20.27	-14.59	1.703		166.67
	VQZ-F12	2.446	20.18	-14.46			166.39

Table 8a. Contribution of the post-CCSD corrections to the properties of N- and O-protonated *trans*-HSNO.

Method	Basis set	N-protonated *trans*-HSNO			O-protonated *trans*-HSNO		
		r(S–N), Å	D_0(S–N), kcal/mol	ΔE(H^+ transfer), kcal/mol	r(S–N), Å	D_0(S–N), kcal/mol	ΔE(H^+ transfer), kcal/mol
CCSD	aug-cc-pV(D+d)Z	1.710	66.85	-5.15	1.621	83.62	-7.73
	jul-cc-pV(D+d)Z	1.710	66.69	-4.42	1.622	83.65	-7.18
	jun-cc-pV(D+d)Z	1.712	63.12	-2.63	1.618	81.12	-5.68
	cc-pV(D+d)Z	1.714	62.26	1.09	1.621	79.53	-1.42
	pVDZ	1.713	64.66	-0.90	1.619	81.55	-1.43
	6-31++G**	1.703	67.79	-3.58	1.616	85.20	-7.32
	6-31G**	1.705	66.35	0.41	1.619	83.58	-3.36
	6-31+G(d)	1.703	67.87	-3.61	1.616	85.33	-6.20
	6-31G	1.822	55.64	12.17	1.748	63.18	19.34
	3-21G	1.809	57.59	20.08	1.739	66.60	22.05
	MIDI!	1.766	62.88	12.67	1.674	77.63	11.63
	MIDI	1.895	54.85	20.64	1.837	60.38	27.65
Δ(T)	aug-cc-pV(D+d)Z	0.000	4.29	0.27	0.015	5.03	0.23
	jul-cc-pV(D+d)Z	0.000	4.29	0.38	0.015	5.03	0.34
	jun-cc-pV(D+d)Z	-0.001	3.97	0.29	0.015	4.69	0.21
	cc-pV(D+d)Z	-0.001	3.69	0.59	0.014	4.44	0.49
	pVDZ	-0.001	3.70	0.25	0.013	4.35	0.31
	6-31++G**	-0.001	4.06	-0.13	0.015	4.59	0.03
	6-31G**	-0.001	3.77	0.05	0.014	4.31	0.22
	6-31+G(d)	-0.001	4.01	-0.02	0.015	4.51	0.20
	6-31G	-0.003	2.73	1.23	0.020	3.24	0.27
	3-21G	-0.005	2.54	1.17	0.020	3.03	0.03
	MIDI!	0.000	3.27	0.83	0.013	4.51	0.39
	MIDI	-0.003	2.09	1.37	0.012	3.56	-0.57
Δ(Q)	cc-pV(D+d)z	0.007	0.81	0.35	0.005	0.61	0.80
	MIDI!	0.008	0.91	0.30	0.006	0.72	0.67
ΔCV	cc-pCVDZ-F12	-0.001	-0.22	0.03	-0.001	-0.27	0.19
	cc-pCVTZ-F12	-0.003	0.16	-0.07	-0.004	0.10	0.10

Table 8b. Contribution of the post-CCSD corrections to the properties of S-protonated and deprotonated trans-HSNO.

Method	Basis set	S-protonated *trans*-HSNO			Deprotonated *trans*-HSNO		
		r(S–N), Å	D_0(S–N), kcal/mol	ΔE(H^+ transfer), kcal/mol	*r*(S–N), Å	D_0(S–N), kcal/mol	ΔE(H^+ transfer), kcal/mol
CCSD	aug-cc-pV(D+d)Z	2.542	17.79	-18.32	1.734	36.34	169.09
	jul-cc-pV(D+d)Z	2.539	17.99	-17.73	1.734	36.34	168.19
	jun-cc-pV(D+d)Z	2.573	16.41	-18.87	1.730	34.83	169.44
	cc-pV(D+d)Z	2.565	16.96	-16.48	1.750	35.14	177.75
	pVDZ	2.554	19.25	-15.23	1.722	43.19	178.45
	6-31++G**	2.509	18.29	-13.09	1.717	38.51	166.54
	6-31G**	2.521	17.92	-9.96	1.738	36.63	171.63
	6-31+G(d)	2.494	19.10	-12.16	1.717	38.51	164.88
	6-31G	2.513	20.64	7.54	1.878	28.64	152.11
	3-21G	2.509	20.70	16.37	1.876	29.47	148.23
	MIDI!	2.411	21.51	-11.16	1.776	42.98	181.97
	MIDI	2.412	22.87	9.13	1.893	39.28	165.15
Δ(T)	aug-cc-pV(D+d)Z	-0.079	3.04	0.55	0.012	5.98	-0.45
	jul-cc-pV(D+d)Z	-0.078	3.08	0.67	0.012	5.98	-0.63
	jun-cc-pV(D+d)Z	-0.082	2.74	0.52	0.011	5.30	-0.25
	cc-pV(D+d)Z	-0.069	2.52	0.76	0.014	4.73	0.63
	pVDZ	-0.058	2.72	0.19	0.012	4.61	0.49
	6-31++G**	-0.067	3.11	-0.11	0.010	5.06	-0.66
	6-31G**	-0.063	2.87	0.00	0.012	4.39	0.16
	6-31+G(d)	-0.060	3.22	-0.15	0.010	5.06	-0.77
	6-31G	-0.022	2.56	-0.03	0.015	3.41	0.60
	3-21G	-0.030	2.28	0.13	0.013	3.13	0.87
	MIDI!	-0.033	2.75	0.46	0.011	4.66	0.43
	MIDI	-0.008	2.31	-0.17	0.008	3.24	0.74
Δ(Q)	cc-pV(D+d)z	-0.007	0.54	0.65	0.017	1.15	0.43
	MIDI!	-0.003	0.48	0.83	0.016	1.28	0.19
ΔCV	cc-pCVDZ-F12	0.000	-0.03	0.24	-0.002	-0.20	-0.16
	cc-pCVTZ-F12	-0.001	-0.01	0.34	-0.004	0.09	-0.09

It is clear that the change of protonation state alternates the properties of HSNO molecule. Based on calculated earlier *S* value (sun of unsigned relative deviations, %), the optimal method, approaching CCSD(T)/CBS quality with moderate computational cost, is CCSD(T_{sc})-F12c/VQZ-F12; and corresponding values of S-N bond lengths and

energies will be used as the reference in this paper. Accounting for the CCSDT(Q) corrections and core-valence correlation was also performed (Tables 7 and 8). Anharmonic vibrational frequencies and corresponding ZPEs are shown in Tables 5 and 6. CCSD(T)-F12a/VQZ-F12 energies were used to calculate BDEs.

It was found that the most favorable energetically pathway is the transfer of proton from H_3O^+ to the S atom of HSNO in comparison to the s transfer to O and N atoms (Figure 5): it decreases in energy by 16.82 kcal/mol (with anharmonic ZPE correction) in comparison to decrease by 7.11 and 4.84 kcal/mol, respectively. The most basic, therefore, is the S atom, and protonation at that position was, most probably, observed in the experiment of Filipovic et al. (Filipovic et al., 2012). Deprotonation of the HSNO molecule is an energetically demanding reaction, with estimated energy increase of the system by 169.67 kcal/mol.

Associated with the proton transfer reaction geometric changes are most pronounced for the S–N bond lengths. Protonation of the S atom leads to significant elongation of the S–N bond in *trans*-HSNO: from 1.865 Å in neutral molecule to 2.437 Å in protonated state. Protonation of the O and N atoms, on the contrary, leads to the shortening of S–N bond to 1.607 Å and 1.683 Å, respectively. Scheme 1 provides an explanation of SNO group behavior upon interaction with Lewis acids: coordination of Lewis acid at S atom increases the weight of resonance structure I (with elongated ionic S-N bond), and coordination of LA at N and O atoms increases the weight of structure D (with shortened double S-N bond).

Also, S-protonation causes the most pronounced conformation change of *trans*-HSNO molecule (Figure 5): elongated S–N bond virtually separates H_2S and NO^+ fragments to form a non-covalent looking structure. Similarly, recent study of HOON (Crabtree et al., 2013; Talipov, Timerghazin, Safiullin, & Khursan, 2013) molecule shows that the presence of elongated and weak O-O bond (1.89 Å, 8.0 kcal/mol BDE) leads to the significant non-covalent character of bonding. Protonation at O and N positions preserves the planarity of the SNO group in *trans*-HSNO.

S–N BDEs are in somewhat logical agreement agreement with the S-N bond lengths: neutral *trans*-HSNO BDE of 33.10 kcal/mol is decreased to 19.52 kcal/mol upon protonation at S atom (calculated with H_2S and NO^+ as dissociation products), and increased to 91.19 and 72.24 kcal/mol upon protonation at O and N atoms, respectively. Therefore, one of the possible mechanisms of activating the HSNO molecule in biologically relevant reactions can start from the protonation at S position. The present study, however, does not account for the solvent effects. Detailed study of the influence of the reaction medium will be presented elsewhere.

VII. Benchmarking of the Commonly Used DFT Methods

Table 9 shows reference values, summarizing the results of accurate *ab initio* calculations. Raw DFT values of S-N bond lengths and energetic parameters are shown in Tables S12-S19 in Supporting Information.

Table 9. Reference data for the DFT methods benchmarking.

Molecule	Parameter	CCSD(T)/ CBS	CCSD(T)/ F12x	Δ(Q)	ΔCV	ΔZPE	Recommended value
Trans-HSNO	r(S–N), Å	1.837*	-	0.033	-0.005	-	1.865
	D_0(S–N), kcal/mol	31.72*	-	1.42	-0.04	-2.79	30.30
Cis-HSNO	r(S–N), Å	1.821*	-	0.035	-0.005	-	1.851
	ΔE(*trans-cis*), kcal/mol	-0.90*	-	-0.11	0.01	0.13	-0.87
HSNO isomerization TS	r(S–N), Å	2.012*	-	0.025	-0.007	-	2.030
	$\Delta E^{\neq}$, kcal/mol	8.99*	-	0.50	0.08	-0.83	8.74
N-protonated *trans*-HSNO	r(S–N), Å	-	1.679	0.007	-0.003	-	1.683
	D_0(S–N), kcal/mol	-	76.34**	0.81	0.16	-5.64**	71.66
	ΔE(H^+ transf.), kcal/mol	-	-5.14	0.35	-0.07	0.32	-4.55
O-protonated *trans*-HSNO	r(S–N), Å	-	1.606	0.005	-0.004	-	1.607
	D_0(S–N), kcal/mol	-	95.45**	0.61	0.20	-5.78**	90.49
	ΔE(H^+ transf.), kcal/mol	-	-7.98	0.80	0.10	0.37	-6.71
S-protonated *trans*-HSNO	r(S–N), Å	-	2.446	-0.007	-0.001	-	2.437
	D_0(S–N), kcal/mol	-	20.18	0.54	-0.01	-1.55	19.16
	ΔE(H^+ transf.), kcal/mol	-	-14.46	0.65	0.34	-3.26	-16.73
Deprotonated *trans*-HSNO	r(S–N), Å	-	1.704	0.017	-0.004	-	1.716
	D_0(S–N), kcal/mol	-	47.33**	1.15	0.09	-0.98**	47.58
	ΔE(H^+ transf.), kcal/mol	-	166.39	0.43	-0.09	2.72	169.45

* (Ivanova et al., 2014)
** CCSD(T)-F12a/VQZ-F12

Analysis of the RMSDs for the S-N bond lengths, as well as the energetic parameters, reveals the differences in performance of DFT functionals, located on different rungs of "Jacob's ladder" (Mardirossian & Head-Gordon, 2014).

In general, S-N bonds are best reproduced with hybrid GGA functionals (rung 4) and hybrid double hybrids (rung 5). The only exception is represented by pure meta-GGA functional N12 (rung 3), which performs the best with Turbomole basis set family in terms of S-N bond length representation. Double-hybrid functionals (rung 5) show the

most robust performance, but are at times preceded by selected hybrid GGAs. Energetic parameters behave similarly. Hybrid meta-GGAs perform among the best, especially ωB97. Double-hybrid functionals are the second best choice, followed by hybrid GGAs. B3P86 functional, recommended in (Baciu & Gauld, 2003), shows good performance representing S-N bond lengths, but only average performance for the energies. PBE0 shows robust performance for both S-N bond lengths and the energies, although not the best in each category. Dispersion-corrected versions of PBE0 (PBE0-GD3 and PBE0-GD3BJ) demonstrate similar results.

Basis set dependence, less pronounced for DFT methods in comparison to *ab initio* ones, was found to be significant for the HSNO system. Using double-ζ quality basis set may be desirable for larger biochemical systems, and in this case Jensen's basis set aug-pcseg-1 performs reasonably well.

Overall, the most robust results in each category were obtained with double-hybrid MPW2PLYPD functional with dispersion correction. This method will be used in the future studies of the mechanisms of biologically relevant reactions of RSNOs.

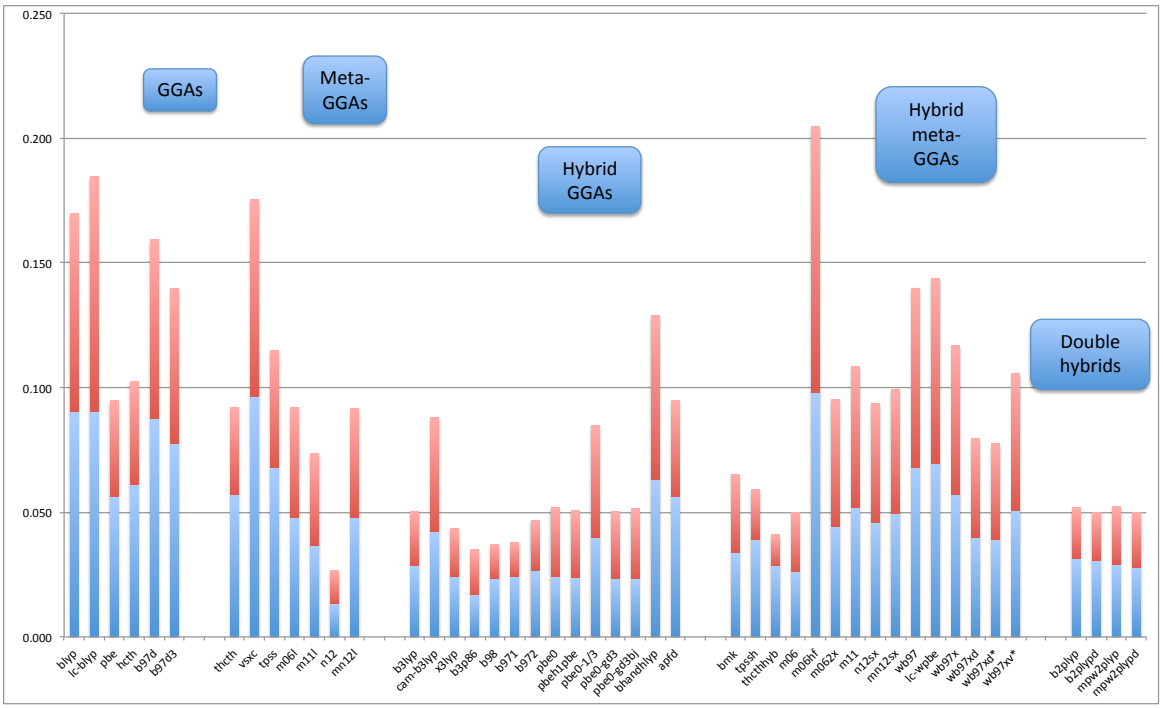

Figure 6. RMSDs for the S-N bond lengths (Å), calculated with def2-SV(P)+d (shown in red) and def2-TZVPPD (shown in blue) basis sets.

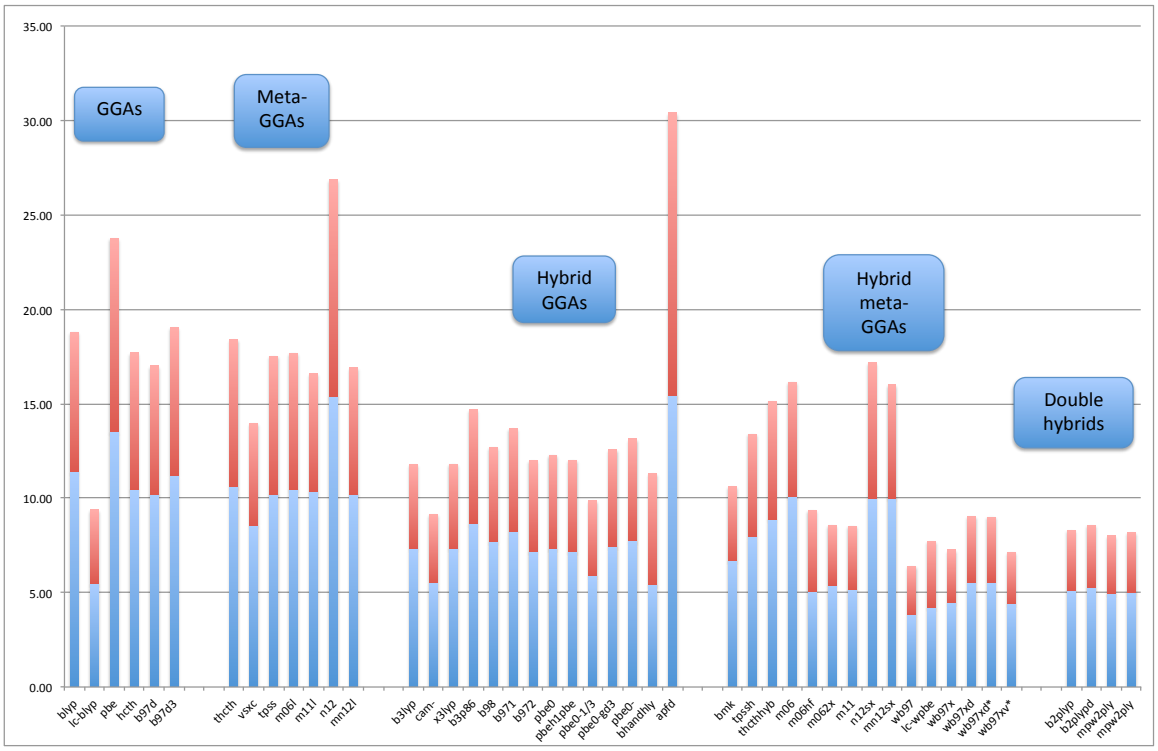

Figure 7. RMSDs for the energetic parameters (kcal/mol), calculated with def2-SV(P)+d (shown in red) and def2-TZVPPD (shown in blue) basis sets.

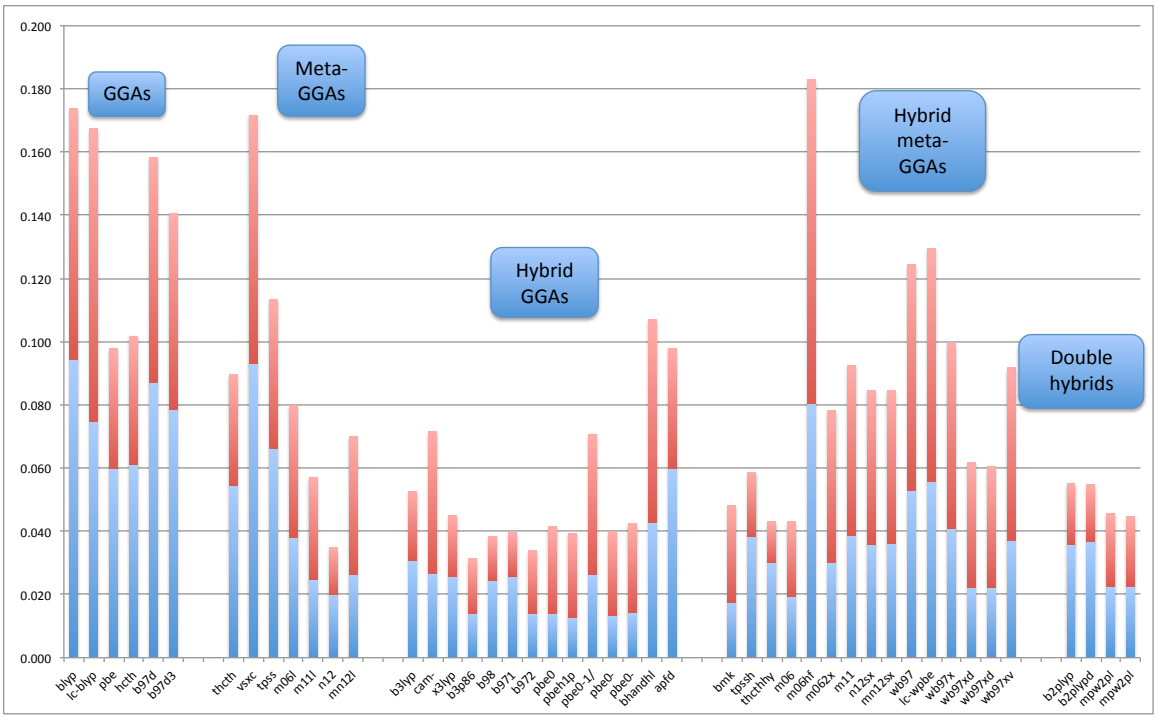

Figure 8. RMSDs for the S-N bond lengths (Å), calculated with aug-pcseg-1 (shown in red) and aug-pcseg-2 (shown in blue) basis sets.

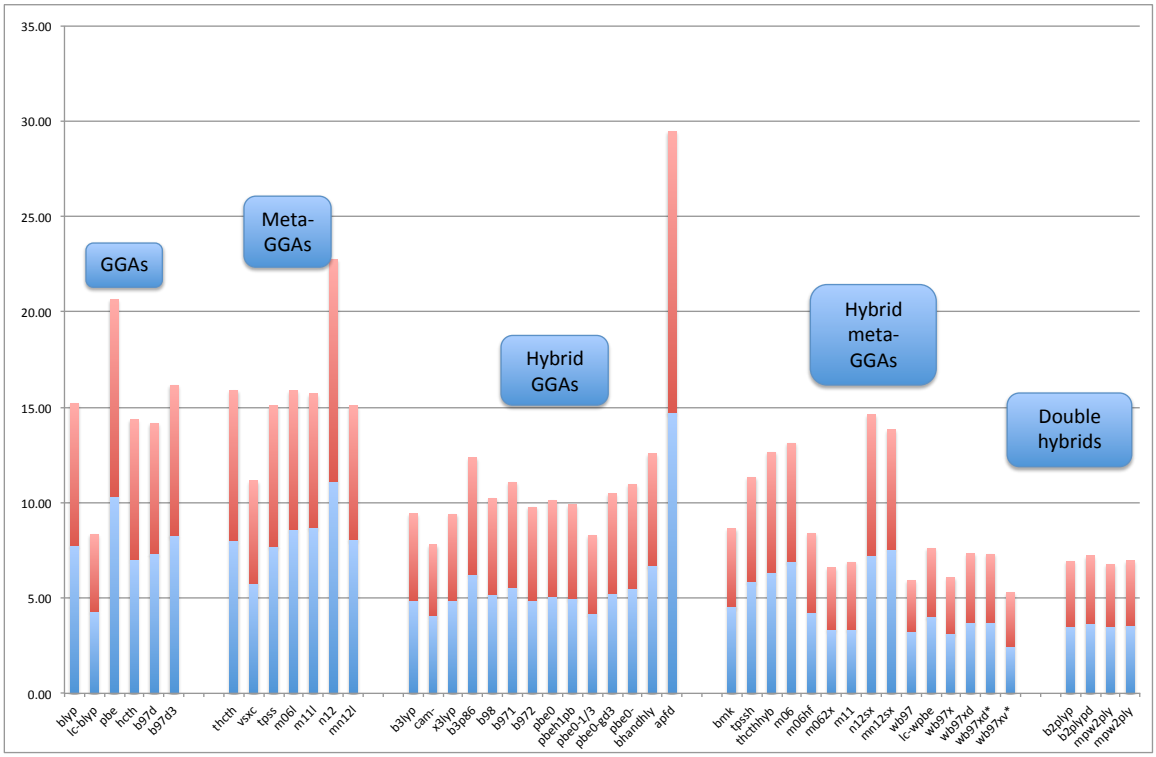

Figure 9. RMSDs for the energetic parameters (kcal/mol), calculated with aug-pcseg-1 (shown in red) and aug-pcseg-2 (shown in blue) basis sets.

Conclusions

In this work, more computationally efficient *ab initio* approach was developed and tested for the simplest S-nitrosothiol, HSNO. First of all, explicitly correlated coupled cluster methods CCSD(T)-F12x were shown to significantly improve the basis set convergence for the HSNO molecule properties in comparison to traditional coupled cluster method CCSD(T). Secondly, multi-electron basis set size, or high-level excitations in coupled cluster theory (perturbative triple and quadruple excitations) were found to be less dependent on the basis set size, and, therefore, can be approximated for the HSNO system and larger systems at affordable computational cost using smaller basis sets MIDI!. Moreover, core-valence correlation energy can also be efficiently approximated with explicitly correlated coupled cluster method with faster basis set convergence in comparison to conventional coupled cluster method. Additional improvement is provided by accounting for the anharmonicity of HSNO vibrational modes, which can be approximated with explicitly correlated coupled cluster theory. All abovementioned effects are crucial for an accurate modeling of spectroscopic or thermochemical properties of S-nitrosothiols.

HSNO molecule in gas phase was shown to have an increased basicity of the S atom in comparison to N and O atoms, with associated changes of the S-N bond properties: protonation at O and N atoms leads to shortening and increase in strength of the S-N bond, when protonation at S atom leads to elongation and weakening of the S-N bond. Deprotonation of HSNO molecule is thermodynamically unfavorable in gas phase, and leads to shortening of the S-N bond with increase of its strength.

Performance of more approximate DFT methods, was tested using reference data, obtained with improved *ab initio* methodology. MPW2PLYPD functional provides both robustness and moderate computational cost for calculating the properties of larger than HSNO S-nitrosothiols and studying the mechanisms of corresponding reactions.

Supporting Information

Table S1. DFT functionals used.

Abbreviation	Reference	Pure/Hybrid	GGA/meta-GGA	Dispersion
BLYP	(Becke 1988; Lee, Yang, & Parr, 1988)	Pure	GGA	No
LC-BLYP	(Iikura, Tsuneda, Yanai, & Hirao, 2001)	Pure	GGA	No
PBE	(Perdew, Burke, & Ernzerhof, 1996; Perdew, Burke, & Wang, 1996)	Pure	GGA	No
HCTH	(Boese & Handy, 2001; Boese, Doltsinis, Handy, & Sprik, 2000; Hamprecht, Cohen, Tozer, & Handy, 1998)	Pure	GGA	No
B97D	(Becke, 1997; Grimme, 2006)	Pure	GGA	Yes
B97D3	(Becke, 1997; Grimme, Ehrlich, & Goerigk, 2011)	Pure	GGA	Yes
tHCTH	(Boese & Handy, 2002)	Pure	Meta-GGA	No
VSXC	(Van Voorhis & Scuseria, 1998)	Pure	Meta-GGA	No
TPSS	(Tao, Perdew, Staroverov, & Scuseria, 2003)	Pure	Meta-GGA	No
M06L	(Zhao & Truhlar, 2006)	Pure	Meta-GGA	No
M11L	(Peverati & Truhlar, 2011)	Pure	Meta-GGA	No
N12	(Peverati & Truhlar, 2012)	Pure	Meta-GGA	No
MN12L	(Peverati & Truhlar, 2012)	Pure	Meta-GGA	No
B3LYP	(Becke 1993; Lee et al., 1988; Stephens, Devlin, Chabalowski, & Frisch, 1994; Vosko, Wilk, & Nusair, 1980)	Hybrid	GGA	No
CAM-B3LYP	(Yanai, Tew, & Handy, 2004)	Hybrid	GGA	No
X3LYP	(Xu & Goddard, 2004)	Hybrid	GGA	No
B3P86	(Becke, 1993; Perdew 1986)	Hybrid	GGA	No
B98	(Becke, 1997)	Hybrid	GGA	No
B971	(Hamprecht et al., 1998)	Hybrid	GGA	No
B972	(Wilson, Bradley, & Tozer, 2001)	Hybrid	GGA	No
PBE0	(Adamo & Barone, 1999)	Hybrid	GGA	No
PBEh1PBE	(Ernzerhof & Perdew, 1998)	Hybrid	GGA	No
PBE0-1/3	(Guido, Brémond, Adamo, & Cortona, 2013)	Hybrid	GGA	No
PBE0-GD3	(Grimme, Antony, Ehrlich, & Krieg, 2010)	Hybrid	GGA	Yes
PBE0-GD3BJ	(Grimme et al., 2011)	Hybrid	GGA	Yes
BHandHLYP	(Becke 1993; Lee et al., 1988)	Hybrid	GGA	No
APFD	(Austin et al., 2012)	Hybrid	GGA	Yes
BMK	(Boese & Martin, 2004)	Hybrid	Meta-GGA	No
TPSSh	(Tao, Perdew, Staroverov, & Scuseria, 2003b)	Hybrid	Meta-GGA	No
tHCTHhyb	tHCTH (Boese & Handy, 2002)	Hybrid	Meta-GGA	No
M06	(Zhao & Truhlar, 2008)	Hybrid	Meta-GGA	No
M06HF	(Zhao & Truhlar, 2006a, 2006b)	Hybrid	Meta-GGA	No

M062X	(Zhao & Truhlar, 2008)	Hybrid	Meta-GGA	No
M11	(Peverati & Truhlar, 2011)	Hybrid	Meta-GGA	No
N12SX	(Peverati & Truhlar, 2012)	Hybrid	Meta-GGA	No
MN12SX	(Peverati & Truhlar, 2012)	Hybrid	Meta-GGA	No
ωB97	(Chai & Head-Gordon, 2008)	Hybrid	Meta-GGA	No
LC-ωPBE	(Vydrov & Scuseria, 2006; Vydrov, Heyd, Krukau, & Scuseria, 2006; Vydrov, Scuseria, & Perdew, 2007)	Hybrid	Meta-GGA	No
ωB97X	(Chai & Head-Gordon, 2008)	Hybrid	Meta-GGA	No
ωB97XD	(Chai & Head-Gordon, 2008)	Hybrid	Meta-GGA	Yes
ωB97XV	(Mardirossian & Head-Gordon, 2014)	Hybrid	Meta-GGA	Yes
B2PLYP	(Grimme, 2006)	Double-Hybrid	GGA	No
B2PLYPD	(Grimme, 2006)	Double-Hybrid	GGA	Yes
MPW2PLYP	(Schwabe & Grimme, 2006)	Double-Hybrid	GGA	No
MPW2PLYPD	(Schwabe & Grimme, 2006)	Double-Hybrid	GGA	Yes

Table S2. *Trans*-HSNO geometries.

Method	Basis set	*r*(N-O), Å	*r*(S-H), Å	∠S–N-O,°	∠N-S-H, °	∠O-N-S-H,°
CCSD(T)	CBS	1.181*	1.338*	114.47*	90.61*	180.00*
CCSD(T)-F12a	aug-cc-pV(D+d)Z	1.182	1.339	114.47	90.46	180.00
	aug-cc-pV(T+d)Z	1.181	1.338	114.49	90.54	180.00
	aug-cc-pV(Q+d)Z	1.180	1.338	114.48	90.60	180.00
	VDZ-F12	1.182	1.337	114.50	90.42	180.00
	VTZ-F12	1.181	1.338	114.47	90.54	180.00
	VQZ-F12	1.180	1.338	114.46	90.60	180.00
CCSD(T)-F12b	aug-cc-pV(D+d)Z	1.181	1.339	114.47	90.51	180.00
	aug-cc-pV(T+d)Z	1.181	1.338	114.50	90.56	180.00
	aug-cc-pV(Q+d)Z	1.180	1.338	114.49	90.59	180.00
	VDZ-F12	1.182	1.337	114.49	90.46	180.00
	VTZ-F12	1.181	1.338	114.48	90.55	180.00
	VQZ-F12	1.181	1.338	114.47	90.60	180.00
CCSD(T)-F12c	aug-cc-pV(D+d)Z	1.180	1.338	114.45	90.79	180.00
	aug-cc-pV(T+d)Z	1.181	1.338	114.45	90.72	180.00
	aug-cc-pV(Q+d)Z	1.180	1.338	114.47	90.67	180.00
	VDZ-F12	1.181	1.347	114.48	90.70	180.00
	VTZ-F12	1.181	1.338	114.45	90.68	180.00
	VQZ-F12	1.180	1.338	114.44	90.67	180.00
$CCSD(T_{sc})$-F12c	aug-cc-pV(D+d)Z	1.180	1.338	114.56	90.58	180.00
	aug-cc-pV(T+d)Z	1.181	1.338	114.49	90.64	180.00
	aug-cc-pV(Q+d)Z	1.180	1.338	114.48	90.63	180.00
	VDZ-F12	1.182	1.337	114.55	90.54	180.00
	VTZ-F12	1.181	1.338	114.48	90.61	180.00
	VQZ-F12	1.180	1.338	114.46	90.63	180.00

* (Ivanova et al., 2014)

Table S3. *Cis*-HSNO geometries.

Method	Basis set	*r*(N-O), Å	*r*(S-H), Å	∠S–N-O,°	∠N-S-H, °	∠O-N-S-H,°
CCSD(T)	CBS	1.184*	1.345*	115.86*	95.41*	0.00*
CCSD(T)-F12a	aug-cc-pV(D+d)Z	1.186	1.346	115.84	95.13	0.00
	aug-cc-pV(T+d)Z	1.185	1.345	115.86	95.31	0.00
	aug-cc-pV(Q+d)Z	1.184	1.345	115.89	95.44	0.00
	VDZ-F12	1.186	1.344	115.86	95.32	0.00
	VTZ-F12	1.185	1.345	115.85	95.34	0.00
	VQZ-F12	1.184	1.345	115.87	95.42	0.00
CCSD(T)-F12b	aug-cc-pV(D+d)Z	1.184	1.346	115.89	95.27	0.00
	aug-cc-pV(T+d)Z	1.185	1.345	115.90	95.38	0.00
	aug-cc-pV(Q+d)Z	1.184	1.345	115.90	95.44	0.00
	VDZ-F12	1.186	1.344	115.88	95.39	0.00
	VTZ-F12	1.185	1.345	115.87	95.37	0.00
	VQZ-F12	1.184	1.345	115.88	95.42	0.00
CCSD(T)-F12c	aug-cc-pV(D+d)Z	1.184	1.345	115.97	95.54	0.00
	aug-cc-pV(T+d)Z	1.185	1.345	115.90	95.48	0.00
	aug-cc-pV(Q+d)Z	1.184	1.345	115.92	95.49	0.00
	VDZ-F12	1.185	1.344	115.96	95.65	0.00
	VTZ-F12	1.184	1.345	115.88	95.44	0.00
	VQZ-F12	1.184	1.344	115.88	95.44	0.00
$CCSD(T_{sc})$-F12c	aug-cc-pV(D+d)Z	1.184	1.345	115.95	95.36	0.00
	aug-cc-pV(T+d)Z	1.185	1.345	115.93	95.46	0.00
	aug-cc-pV(Q+d)Z	1.184	1.345	115.91	95.47	0.00
	VDZ-F12	1.186	1.344	115.93	95.52	0.00
	VTZ-F12	1.185	1.345	115.89	95.42	0.00
	VQZ-F12	1.184	1.345	115.88	95.43	0.00

*(Ivanova et al., 2014)

Table S4. HSNO isomerization TS geometries.

Method	Basis set	*r*(N-O), Å	*r*(S-H), Å	∠S–N-O,°	∠N-S-H, °	∠O-N-S-H,°
CCSD(T)	CBS	1.157*	1.341*	112.95*	87.72*	87.51*
CCSD(T)-F12a	aug-cc-pV(D+d)Z	1.160	1.342	112.95	87.66	87.57
	aug-cc-pV(T+d)Z	1.158	1.341	112.96	87.67	87.53
	aug-cc-pV(Q+d)Z	1.157	1.341	112.95	87.75	87.51
	VDZ-F12	1.159	1.340	112.95	87.62	87.73
	VTZ-F12	1.158	1.341	112.93	87.63	87.60
	VQZ-F12	1.157	1.341	112.93	87.72	87.55
CCSD(T)-F12b	aug-cc-pV(D+d)Z	1.158	1.342	112.96	87.71	87.53
	aug-cc-pV(T+d)Z	1.158	1.341	112.97	87.68	87.51
	aug-cc-pV(Q+d)Z	1.157	1.341	112.96	87.74	87.50
	VDZ-F12	1.158	1.340	112.95	87.67	87.70
	VTZ-F12	1.158	1.341	112.94	87.64	87.58
	VQZ-F12	1.157	1.341	112.94	87.72	87.55
CCSD(T)-F12c	aug-cc-pV(D+d)Z	1.157	1.341	113.01	88.02	87.39
	aug-cc-pV(T+d)Z	1.157	1.341	112.98	87.86	87.46
	aug-cc-pV(Q+d)Z	1.157	1.341	112.96	87.82	87.48
	VDZ-F12	1.158	1.339	113.00	87.93	87.59
	VTZ-F12	1.157	1.341	112.95	87.79	87.53
	VQZ-F12	1.157	1.341	112.94	87.79	87.52
CCSD(T_{sc})-F12c	aug-cc-pV(D+d)Z	1.157	1.341	113.02	87.65	87.50
	aug-cc-pV(T+d)Z	1.157	1.341	112.98	87.73	87.49
	aug-cc-pV(Q+d)Z	1.157	1.341	112.96	87.76	87.49
	VDZ-F12	1.158	1.340	113.00	87.63	87.49
	VTZ-F12	1.157	1.341	112.95	87.67	87.56
	VQZ-F12	1.157	1.341	112.94	87.73	87.54

* (Ivanova et al., 2014)

Table S5. Coupled cluster method diagnostic values for neutral HSNO.

Method	Basis set	*trans*-HSNO			*cis*-HSNO			HSNO isomerization TS		
		T1	D1	Largest T2 amplitude	T1	D1	Largest T2 amplitude	T1	D1	Largest T2 amplitude
CCSD(T)-F12a	aug-cc-pV(D+d)Z	0.027	0.078	0.092	0.027	0.075	0.090	0.022	0.071	0.073
	aug-cc-pV(T+d)Z	0.027	0.078	0.084	0.026	0.075	0.082	0.022	0.072	0.083
	aug-cc-pV(Q)+dZ	0.027	0.078	0.072	0.026	0.075	0.068	0.022	0.072	0.086
	VDZ-F12	0.027	0.077	0.086	0.026	0.074	0.083	0.022	0.070	0.079
	VTZ-F12	0.027	0.078	0.075	0.026	0.075	0.071	0.022	0.071	0.079
	VQZ-F12	0.027	0.078	0.060	0.026	0.075	0.068	0.022	0.072	0.056
CCSD(T)-F12b	aug-cc-pV(D+d)Z	0.027	0.078	0.092	0.027	0.075	0.090	0.022	0.071	0.073
	aug-cc-pV(T+d)Z	0.027	0.078	0.084	0.026	0.075	0.082	0.022	0.072	0.083
	aug-cc-pV(Q)+dZ	0.027	0.078	0.072	0.026	0.075	0.068	0.022	0.072	0.086
	VDZ-F12	0.027	0.077	0.086	0.026	0.074	0.086	0.022	0.070	0.079
	VTZ-F12	0.027	0.078	0.075	0.026	0.075	0.071	0.022	0.071	0.079
	VQZ-F12	0.027	0.078	0.060	0.026	0.075	0.068	0.022	0.072	0.056
CCSD(T)-F12c	aug-cc-pV(D+d)Z	0.024	0.069	0.089	0.024	0.067	0.088	0.020	0.064	0.071
	aug-cc-pV(T+d)Z	0.026	0.074	0.083	0.025	0.071	0.081	0.021	0.068	0.082
	aug-cc-pV(Q)+dZ	0.026	0.076	0.071	0.025	0.073	0.068	0.021	0.070	0.085
	VDZ-F12	0.025	0.071	0.085	0.024	0.068	0.082	0.020	0.065	0.078
	VTZ-F12	0.026	0.074	0.074	0.025	0.072	0.070	0.021	0.069	0.078
	VQZ-F12	0.026	0.076	0.060	0.026	0.074	0.067	0.021	0.070	0.055
CCSD(T_{sc})-F12c	aug-cc-pV(D+d)Z	0.024	0.069	0.089	0.024	0.067	0.088	0.020	0.064	0.071
	aug-cc-pV(T+d)Z	0.026	0.074	0.083	0.025	0.071	0.081	0.021	0.068	0.082
	aug-cc-pV(Q)+dZ	0.026	0.076	0.071	0.025	0.073	0.068	0.021	0.070	0.085
	VDZ-F12	0.025	0.071	0.085	0.024	0.068	0.082	0.020	0.065	0.078
	VTZ-F12	0.026	0.074	0.074	0.025	0.072	0.070	0.021	0.069	0.078
	VQZ-F12	0.026	0.076	0.060	0.026	0.074	0.067	0.021	0.070	0.055

Table S6. Coupled cluster method diagnostic values for protonated forms of HSNO molecule.

Method	Basis set	N-protonated HSNO			N-protonated HSNO			S-protonated HSNO		
		T1	D1	Largest T2 amplitude	T1	D1	Largest T2 amplitude	T1	D1	Largest T2 amplitude
CCSD(T)-F12a	aug-cc-pV(D+d)Z	0.026	0.087	0.097	0.025	0.091	0.109	0.020	0.067	0.104
	aug-cc-pV(T+d)Z	0.025	0.081	0.095	0.024	0.087	0.107	0.019	0.064	0.102
	VDZ-F12	0.026	0.087	0.097	0.025	0.090	0.108	0.020	0.066	0.104
	VTZ-F12	0.025	0.081	0.095	0.024	0.087	0.107	0.019	0.064	0.102
CCSD(T)-F12b	aug-cc-pV(D+d)Z	0.026	0.087	0.097	0.025	0.091	0.106	0.020	0.067	0.104
	aug-cc-pV(T+d)Z	0.025	0.081	0.095	0.024	0.087	0.104	0.019	0.064	0.102
	VDZ-F12	0.026	0.087	0.097	0.025	0.090	0.105	0.020	0.066	0.104
	VTZ-F12	0.025	0.081	0.095	0.024	0.087	0.104	0.019	0.064	0.102
CCSD(T)-F12c	aug-cc-pV(D+d)Z	0.023	0.075	0.095	0.023	0.082	0.101	0.018	0.060	0.102
	aug-cc-pV(T+d)Z	0.024	0.077	0.094	0.024	0.084	0.102	0.019	0.061	0.101
	VDZ-F12	0.024	0.077	0.096	0.023	0.084	0.102	0.018	0.062	0.102
	VTZ-F12	0.024	0.078	0.095	0.024	0.084	0.102	0.019	0.062	0.101
CCSD(T_{sc})-F12c	aug-cc-pV(D+d)Z	0.023	0.075	0.095	0.023	0.082	0.101	0.018	0.060	0.101
	aug-cc-pV(T+d)Z	0.024	0.077	0.094	0.024	0.084	0.102	0.019	0.061	0.101
	VDZ-F12	0.024	0.077	0.096	0.023	0.084	0.102	0.018	0.062	0.102
	VTZ-F12	0.024	0.078	0.095	0.024	0.084	0.102	0.019	0.062	0.101

Table S7. Coupled cluster method diagnostic values for deprotonated HSNO molecule.

Method	Basis set	T1	D1	Largest T2 amplitude
CCSD(T)-F12a	aug-cc-pV(D+d)Z	0.030	0.095	0.055
	aug-cc-pV(T+d)Z	0.029	0.093	< 0.05
	VDZ-F12	0.030	0.096	0.054
	VTZ-F12	0.029	0.094	< 0.05
CCSD(T)-F12b	aug-cc-pV(D+d)Z	0.030	0.095	0.055
	aug-cc-pV(T+d)Z	0.029	0.093	< 0.05
	VDZ-F12	0.030	0.096	0.054
	VTZ-F12	0.029	0.094	< 0.05
CCSD(T)-F12c	aug-cc-pV(D+d)Z	0.027	0.085	0.053
	aug-cc-pV(T+d)Z	0.028	0.089	< 0.05
	VDZ-F12	0.027	0.088	0.052
	VTZ-F12	0.028	0.090	< 0.05
CCSD(T_{sc})-F12c	aug-cc-pV(D+d)Z	0.027	0.085	0.053
	aug-cc-pV(T+d)Z	0.028	0.089	< 0.05
	VDZ-F12	0.027	0.088	0.052
	VTZ-F12	0.028	0.090	< 0.05

Table S8. Unsigned relative deviations (%) from CCSD(T)/CBS data for *trans*-HSNO.

Method	Basis set	r(S–N)	r(N-O)	r(S-H)	∠S–N-O	∠N-S-H	D_0(S–N)
CCSD(T)-F12a	aug-cc-pV(D+d)Z	0.054	0.085	0.075	0.003	0.166	3.052
	aug-cc-pV(T+d)Z	0.109	0.000	0.000	0.015	0.073	0.534
	aug-cc-pV(Q+d)Z	0.054	0.085	0.000	0.009	0.014	0.793
	VDZ-F12	0.054	0.085	0.075	0.022	0.212	0.929
	VTZ-F12	0.109	0.000	0.000	0.003	0.081	0.938
	VQZ-F12	0.054	0.085	0.000	0.007	0.014	0.931
CCSD(T)-F12b	aug-cc-pV(D+d)Z	0.054	0.000	0.075	0.001	0.109	1.369
	aug-cc-pV(T+d)Z	0.054	0.000	0.000	0.022	0.056	1.218
	aug-cc-pV(Q+d)Z	0.054	0.085	0.000	0.018	0.018	1.206
	VDZ-F12	0.054	0.085	0.075	0.016	0.168	0.209
	VTZ-F12	0.054	0.000	0.000	0.010	0.065	1.601
	VQZ-F12	0.000	0.000	0.000	0.003	0.007	1.324
CCSD(T)-F12c	aug-cc-pV(D+d)Z	0.569	0.056	0.010	0.018	0.199	-
	aug-cc-pV(T+d)Z	0.257	0.008	0.002	0.016	0.118	
	aug-cc-pV(Q+d)Z	0.115	0.058	0.007	0.004	0.065	
	VDZ-F12	0.397	0.039	0.663	0.004	0.094	
	VTZ-F12	0.199	0.029	0.016	0.017	0.076	
	VQZ-F12	0.109	0.056	0.024	0.024	0.063	
CCSD(T_{sc})-F12c	aug-cc-pV(D+d)Z	0.142	0.045	0.034	0.080	0.036	-
	aug-cc-pV(T+d)Z	0.084	0.002	0.016	0.017	0.034	
	aug-cc-pV(Q+d)Z	0.028	0.057	0.003	0.010	0.024	
	VDZ-F12	0.062	0.067	0.067	0.067	0.078	
	VTZ-F12	0.033	0.025	0.007	0.010	0.002	
	VQZ-F12	0.017	0.058	0.019	0.008	0.020	

Table S9. Unsigned relative deviations (%) from CCSD(T)/CBS data for *cis*-HSNO.

Method	Basis set	*r*(S–N)	*r*(N-O)	*r*(S-H)	∠S–N-O	∠N-S-H	ΔE(*trans*-*cis*, EE)
CCSD(T)-F12a	aug-cc-pV(D+d)Z	0.000	0.169	0.074	0.021	0.295	0.579
	aug-cc-pV(T+d)Z	0.000	0.084	0.000	0.003	0.101	1.243
	aug-cc-pV(Q+d)Z	0.055	0.000	0.000	0.023	0.027	0.912
	VDZ-F12	0.055	0.169	0.074	0.001	0.091	2.405
	VTZ-F12	0.000	0.084	0.000	0.010	0.079	1.288
	VQZ-F12	0.055	0.000	0.000	0.007	0.006	0.256
CCSD(T)-F12b	aug-cc-pV(D+d)Z	0.055	0.000	0.074	0.024	0.149	2.104
	aug-cc-pV(T+d)Z	0.055	0.084	0.000	0.031	0.035	2.014
	aug-cc-pV(Q+d)Z	0.055	0.000	0.000	0.038	0.035	1.580
	VDZ-F12	0.110	0.169	0.074	0.019	0.017	3.323
	VTZ-F12	0.055	0.084	0.000	0.011	0.045	2.021
	VQZ-F12	0.055	0.000	0.000	0.018	0.005	0.472
CCSD(T)-F12c	aug-cc-pV(D+d)Z	0.624	0.008	0.008	0.096	0.139	1.184
	aug-cc-pV(T+d)Z	0.270	0.042	0.015	0.033	0.070	0.789
	aug-cc-pV(Q+d)Z	0.138	0.007	0.024	0.051	0.082	0.254
	VDZ-F12	0.496	0.121	0.089	0.084	0.250	0.220
	VTZ-F12	0.187	0.024	0.036	0.019	0.031	0.024
	VQZ-F12	0.092	0.011	0.042	0.018	0.028	0.479
$CCSD(T_{sc})$-F12c	aug-cc-pV(D+d)Z	0.158	0.030	0.021	0.079	0.051	0.140
	aug-cc-pV(T+d)Z	0.130	0.073	0.005	0.057	0.055	0.281
	aug-cc-pV(Q+d)Z	0.102	0.021	0.009	0.046	0.064	0.511
	VDZ-F12	0.134	0.160	0.070	0.062	0.113	0.944
	VTZ-F12	0.107	0.057	0.020	0.025	0.015	0.565
	VQZ-F12	0.058	0.013	0.031	0.017	0.017	0.057

Table S10. Unsigned relative deviations (%) from CCSD(T)/CBS data for HSNO isomerization TS.

Method	Basis set	r(S–N)	r(N-O)	r(S-H)	∠S–N-O	∠N-S-H	∠O-N-S-H	$\Delta E^{\neq}$ (EE)
CCSD(T)-F12a	aug-cc-pV(D+d)Z	0.348	0.259	0.075	0.004	0.064	0.066	1.721
	aug-cc-pV(T+d)Z	0.000	0.086	0.000	0.004	0.062	0.021	0.333
	aug-cc-pV(Q+d)Z	0.000	0.000	0.000	0.000	0.034	0.002	0.234
	VDZ-F12	0.149	0.173	0.075	0.002	0.119	0.248	1.660
	VTZ-F12	0.050	0.086	0.000	0.018	0.104	0.097	0.050
	VQZ-F12	0.000	0.000	0.000	0.014	0.000	0.048	0.035
CCSD(T)-F12b	aug-cc-pV(D+d)Z	0.249	0.086	0.075	0.010	0.015	0.019	2.356
	aug-cc-pV(T+d)Z	0.050	0.086	0.000	0.015	0.048	0.005	0.658
	aug-cc-pV(Q+d)Z	0.050	0.000	0.000	0.009	0.027	0.010	0.432
	VDZ-F12	0.149	0.086	0.075	0.003	0.059	0.222	2.467
	VTZ-F12	0.000	0.086	0.000	0.009	0.089	0.079	0.327
	VQZ-F12	0.050	0.000	0.000	0.010	0.002	0.043	0.168
CCSD(T)-F12c	aug-cc-pV(D+d)Z	0.950	0.018	0.012	0.057	0.342	0.139	3.252
	aug-cc-pV(T+d)Z	0.317	0.038	0.010	0.026	0.161	0.063	1.061
	aug-cc-pV(Q+d)Z	3.787	0.002	0.013	0.012	0.113	0.038	0.545
	VDZ-F12	0.542	0.094	0.114	0.048	0.241	0.096	2.168
	VTZ-F12	0.250	0.021	0.025	0.002	0.075	0.019	0.499
	VQZ-F12	0.170	0.003	0.030	0.006	0.078	0.014	0.220
CCSD(T_{sc})-F12c	aug-cc-pV(D+d)Z	0.217	0.018	0.021	0.066	0.083	0.016	3.281
	aug-cc-pV(T+d)Z	0.032	0.029	0.012	0.026	0.010	0.025	0.966
	aug-cc-pV(Q+d)Z	0.052	0.002	0.000	0.011	0.042	0.023	0.467
	VDZ-F12	0.022	0.091	0.080	0.045	0.103	0.023	2.113
	VTZ-F12	0.012	0.014	0.013	0.001	0.060	0.056	0.357
	VQZ-F12	0.033	0.003	0.022	0.007	0.007	0.029	0.124

Table S11. H_2O proton affinities (EE, kcal/mol).

Method	Basis set	H^+ affinity
CCSD(T)-F12a	aug-cc-pV(D+d)Z	-171.70
	aug-cc-pV(T+d)Z	-171.50
	aug-cc-pV(Q+d)Z	-171.43
	VDZ-F12	-171.70
	VTZ-F12	-171.40
	VQZ-F12	-171.40
CCSD(T)-F12b	aug-cc-pV(D+d)Z	-171.86
	aug-cc-pV(T+d)Z	-171.63
	aug-cc-pV(Q+d)Z	-171.53
	VDZ-F12	-171.88
	VTZ-F12	-171.49
	VQZ-F12	-171.45
CCSD(T)-F12c	aug-cc-pV(D+d)Z	-172.01
	aug-cc-pV(T+d)Z	-171.70
	aug-cc-pV(Q+d)Z	-171.55
	VDZ-F12	-171.89
	VTZ-F12	-171.55
	VQZ-F12	-171.49
$CCSD(T_{sc})$-F12c	aug-cc-pV(D+d)Z	-171.85
	aug-cc-pV(T+d)Z	-171.62
	aug-cc-pV(Q+d)Z	-171.51
	VDZ-F12	-171.76
	VTZ-F12	-171.48
	VQZ-F12	-171.45

Table S12. S-N bond length values (Å), calculated with different DFT methods (with def2-SV(P)+d basis set).

Method	*Trans*-HSNO	*Cis*-HSNO	HSNO isomerization TS	N-prot. HSNO	O-prot. HSNO	S-prot. HSNO	Deprot. HSNO
B3LYP	1.886	1.859	2.044	1.699	1.610	2.506	1.722
CAM-B3LYP	1.816	1.787	1.966	1.685	1.594	2.473	1.694
B3P86	1.858	1.830	2.013	1.688	1.602	2.472	1.711
B98	1.882	1.859	2.032	1.695	1.606	2.495	1.719
B971	1.884	1.861	2.033	1.696	1.608	2.497	1.722
B972	1.862	1.835	2.024	1.689	1.601	2.506	1.712
X3LYP	1.877	1.849	2.035	1.697	1.608	2.499	1.718
BMK	1.853	1.833	1.977	1.673	1.585	2.494	1.686
TPSSh	1.913	1.894	2.067	1.703	1.615	2.504	1.735
BHandHLYP	1.792	1.765	1.939	1.681	1.583	2.511	1.685
tHCTHhyb	1.897	1.876	2.047	1.696	1.608	2.497	1.725
PBEh1PBE	1.847	1.818	2.004	1.685	1.599	2.479	1.707
PBE0	1.846	1.816	2.000	1.685	1.599	2.475	1.706
PBE0-1/3	1.819	1.790	1.973	1.678	1.591	2.474	1.694
M06	1.848	1.825	1.997	1.696	1.607	2.488	1.715
M06HF	1.753	1.738	1.847	1.692	1.577	2.515	1.679
M062X	1.815	1.792	1.957	1.688	1.593	2.480	1.696
ωB97XD	1.822	1.795	1.977	1.683	1.595	2.491	1.697
ωB97X	1.798	1.773	1.941	1.681	1.591	2.496	1.688
ωB97	1.787	1.765	1.921	1.680	1.590	2.514	1.686
LC-ωPBE	1.780	1.756	1.912	1.676	1.584	2.482	1.682
M11	1.808	1.783	1.945	1.685	1.592	2.489	1.687
N12SX	1.808	1.776	1.961	1.675	1.589	2.447	1.692
MN12SX	1.806	1.777	1.968	1.676	1.593	2.495	1.688
M06L	1.914	1.900	2.075	1.702	1.614	2.529	1.741
M11L	1.879	1.868	2.050	1.669	1.586	2.525	1.704
VSXC	1.983	1.971	2.135	1.707	1.619	2.592	1.749
HCTH	1.930	1.910	2.092	1.702	1.613	2.553	1.740
tHCTH	1.938	1.921	2.094	1.706	1.615	2.522	1.742
N12	1.871	1.845	2.012	1.680	1.594	2.463	1.712
MN12L	1.833	1.799	2.012	1.675	1.596	2.545	1.699
B97-D	1.982	1.965	2.132	1.723	1.628	2.549	1.762
B97-D3	1.969	1.956	2.117	1.719	1.627	2.532	1.760
TPSS	1.958	1.946	2.101	1.717	1.627	2.517	1.758
PBE	1.944	1.927	2.084	1.716	1.628	2.501	1.757
BLYP	1.986	1.972	2.126	1.732	1.640	2.547	1.775
LC-BLYP	1.751	1.726	1.872	1.670	1.575	2.459	1.668
APFD	1.944	1.927	2.084	1.716	1.628	2.501	1.757
PBE0-GD3	1.846	1.818	2.003	1.686	1.599	2.476	1.706
PBE0-GD3BJ	1.846	1.816	2.000	1.685	1.599	2.472	1.706
B2PLYP	1.881	1.848	2.051	1.688	1.610	2.516	1.712
B2PLYPD	1.884	1.850	2.054	1.689	1.610	2.512	1.712
MPW2PLYP	1.859	1.825	2.027	1.685	1.605	2.508	1.705
MPW2PLYPD	1.860	1.826	2.029	1.686	1.605	2.506	1.705
ωB97XD*	1.825	1.798	1.978	1.683	1.596	2.494	1.697
ωB97XV*	1.807	1.783	1.947	1.687	1.595	2.489	1.696

* QChem 4.2

Table S13. S-N bond length values (Å), calculated with different DFT methods (with def2-TZVPPD basis set).

Method	*Trans*-HSNO	*Cis*-HSNO	HSNO isomeriza-tion TS	N-prot. HSNO	O-prot. HSNO	S-prot. HSNO	Deprot. HSNO
B3LYP	1.872	1.857	2.034	1.694	1.609	2.493	1.716
CAM-B3LYP	1.805	1.786	1.957	1.680	1.594	2.462	1.689
B3P86	1.843	1.825	2.000	1.682	1.602	2.442	1.704
B98	1.865	1.854	2.020	1.690	1.606	2.471	1.714
B971	1.866	1.855	2.020	1.691	1.609	2.470	1.716
B972	1.846	1.830	2.006	1.684	1.602	2.473	1.706
X3LYP	1.862	1.847	2.025	1.692	1.607	2.487	1.713
BMK	1.843	1.831	1.976	1.671	1.586	2.480	1.689
TPSSh	1.886	1.875	2.044	1.696	1.614	2.473	1.724
BHandHLYP	1.784	1.768	1.930	1.676	1.584	2.509	1.685
tHCTHhyb	1.876	1.864	2.030	1.690	1.608	2.465	1.716
PBEh1PBE	1.830	1.812	1.986	1.681	1.600	2.448	1.700
PBE0	1.828	1.811	1.983	1.680	1.600	2.441	1.700
PBE0-1/3	1.805	1.787	1.957	1.674	1.592	2.441	1.690
M06	1.847	1.833	2.002	1.692	1.606	2.487	1.715
M06HF	1.734	1.724	1.830	1.680	1.572	2.489	1.666
M062X	1.800	1.785	1.940	1.682	1.594	2.468	1.691
ωB97XD	1.814	1.795	1.969	1.679	1.596	2.469	1.693
ωB97X	1.789	1.772	1.931	1.677	1.592	2.482	1.686
ωB97	1.776	1.761	1.908	1.676	1.591	2.499	1.682
LC-ωPBE	1.768	1.753	1.900	1.671	1.585	2.449	1.676
M11	1.791	1.773	1.934	1.677	1.588	2.452	1.680
N12SX	1.803	1.782	1.957	1.673	1.590	2.411	1.685
MN12SX	1.800	1.782	1.959	1.670	1.593	2.484	1.688
M06L	1.907	1.904	2.070	1.698	1.615	2.519	1.738
M11L	1.873	1.872	2.051	1.659	1.585	2.524	1.710
VSXC	1.946	1.940	2.109	1.701	1.620	2.587	1.738
HCTH	1.903	1.894	2.067	1.697	1.616	2.521	1.728
tHCTH	1.908	1.900	2.070	1.697	1.615	2.485	1.729
N12	1.862	1.848	2.009	1.676	1.596	2.419	1.700
MN12L	1.829	1.810	2.000	1.671	1.597	2.532	1.701
B97-D	1.959	1.952	2.113	1.715	1.628	2.523	1.752
B97-D3	1.947	1.943	2.101	1.712	1.627	2.506	1.750
TPSS	1.927	1.923	2.079	1.709	1.626	2.484	1.743
PBE	1.919	1.910	2.065	1.710	1.628	2.464	1.743
BLYP	1.967	1.963	2.115	1.726	1.638	2.530	1.763
LC-BLYP	1.743	1.726	1.866	1.666	1.574	2.457	1.664
APFD	1.919	1.910	2.065	1.710	1.628	2.464	1.743
PBE0-GD3	1.830	1.813	1.985	1.681	1.600	2.442	1.700
PBE0-GD3BJ	1.828	1.811	1.982	1.680	1.600	2.438	1.700
B2PLYP	1.867	1.848	2.039	1.683	1.611	2.490	1.707
B2PLYPD	1.870	1.850	2.042	1.683	1.611	2.487	1.708
MPW2PLYP	1.846	1.826	2.015	1.680	1.605	2.486	1.701
MPW2PLYPD	1.848	1.827	2.017	1.680	1.605	2.484	1.701
ωB97XD*	1.816	1.798	1.970	1.679	1.597	2.465	1.694
ωB97XV*	1.794	1.779	1.932	1.682	1.597	2.466	1.691

* QChem 4.2

Table S14. S-N bond length values (Å), calculated with different DFT methods (with aug-pcseg-1 basis set).

Method	*Trans*-HSNO	*Cis*-HSNO	HSNO isomeriza-tion TS	N-prot. HSNO	O-prot. HSNO	S-prot. HSNO	Deprot. HSNO
B3LYP	1.902	1.892	2.047	1.715	1.632	2.469	1.742
CAM-B3LYP	1.836	1.821	1.975	1.698	1.615	2.438	1.713
B3P86	1.873	1.860	2.015	1.701	1.622	2.421	1.728
B98	1.897	1.888	2.034	1.709	1.627	2.451	1.740
B971	1.898	1.889	2.035	1.710	1.629	2.452	1.741
B972	1.877	1.866	2.024	1.701	1.622	2.454	1.729
X3LYP	1.895	1.883	2.040	1.713	1.629	2.465	1.739
BMK	1.866	1.858	1.985	1.687	1.603	2.442	1.714
TPSSh	1.917	1.910	2.059	1.716	1.635	2.455	1.748
BHandHLYP	1.816	1.801	1.952	1.694	1.604	2.479	1.708
tHCTHhyb	1.906	1.898	2.045	1.710	1.630	2.448	1.743
PBEh1PBE	1.862	1.849	2.006	1.699	1.620	2.431	1.723
PBE0	1.860	1.848	2.003	1.698	1.619	2.425	1.723
PBE0-1/3	1.836	1.822	1.976	1.691	1.611	2.423	1.713
M06	1.853	1.841	1.995	1.706	1.625	2.443	1.731
M06HF	1.769	1.762	1.868	1.698	1.594	2.465	1.689
M062X	1.832	1.822	1.966	1.698	1.612	2.439	1.716
ωB97XD	1.842	1.828	1.983	1.695	1.615	2.445	1.715
ωB97X	1.817	1.803	1.950	1.693	1.611	2.456	1.708
ωB97	1.803	1.791	1.928	1.692	1.608	2.475	1.702
LC-ωPBE	1.796	1.783	1.921	1.688	1.603	2.431	1.696
M11	1.820	1.806	1.953	1.693	1.607	2.422	1.701
N12SX	1.828	1.812	1.968	1.690	1.611	2.391	1.708
MN12SX	1.815	1.801	1.966	1.685	1.609	2.435	1.705
M06L	1.910	1.906	2.059	1.710	1.630	2.476	1.755
M11L	1.893	1.896	2.051	1.680	1.605	2.460	1.736
VSXC	1.982	1.979	2.128	1.721	1.640	2.566	1.762
HCTH	1.943	1.938	2.090	1.719	1.637	2.509	1.755
tHCTH	1.941	1.936	2.086	1.719	1.637	2.469	1.754
N12	1.889	1.878	2.018	1.697	1.620	2.408	1.724
MN12L	1.837	1.819	1.998	1.685	1.612	2.482	1.714
B97-D	1.986	1.979	2.124	1.737	1.651	2.502	1.780
B97-D3	1.974	1.971	2.111	1.733	1.649	2.486	1.777
TPSS	1.957	1.954	2.092	1.730	1.648	2.467	1.769
PBE	1.949	1.942	2.080	1.731	1.650	2.452	1.769
BLYP	1.992	1.988	2.125	1.749	1.663	2.510	1.792
LC-BLYP	1.771	1.757	1.887	1.684	1.594	2.427	1.685
APFD	1.949	1.942	2.080	1.731	1.650	2.452	1.769
PBE0-GD3	1.862	1.849	2.005	1.699	1.619	2.426	1.723
PBE0-GD3BJ	1.860	1.847	2.002	1.698	1.619	2.422	1.722
B2PLYP	1.911	1.898	2.066	1.704	1.634	2.480	1.737
B2PLYPD	1.914	1.900	2.069	1.704	1.634	2.477	1.737
MPW2PLYP	1.888	1.873	2.043	1.700	1.627	2.475	1.729
MPW2PLYPD	1.890	1.875	2.045	1.701	1.627	2.473	1.729
ωB97XD*	1.843	1.827	1.984	1.696	1.615	2.447	1.716
ωB97XV*	1.824	1.811	1.954	1.699	1.615	2.449	1.712

* QChem 4.2

Table S15. S-N bond length values (Å), calculated with different DFT methods (with aug-pcseg-2 basis set).

Method	*Trans*-HSNO	*Cis*-HSNO	HSNO isomerization TS	N-prot. HSNO	O-prot. HSNO	S-prot. HSNO	Deprot. HSNO
B3LYP	1.873	1.858	2.033	1.696	1.612	2.492	1.717
CAM-B3LYP	1.807	1.788	1.957	1.682	1.596	2.462	1.691
B3P86	1.844	1.827	1.999	1.685	1.604	2.442	1.705
B98	1.865	1.854	2.019	1.691	1.608	2.471	1.714
B971	1.866	1.855	2.019	1.693	1.611	2.470	1.716
B972	1.846	1.831	2.005	1.685	1.604	2.473	1.707
X3LYP	1.863	1.849	2.024	1.694	1.610	2.487	1.714
BMK	1.841	1.828	1.977	1.674	1.590	2.478	1.691
TPSSh	1.886	1.875	2.043	1.698	1.617	2.474	1.725
BHandHLYP	1.788	1.770	1.930	1.678	1.586	2.508	1.687
tHCTHhyb	1.876	1.865	2.029	1.692	1.610	2.465	1.717
PBEh1PBE	1.831	1.814	1.985	1.682	1.602	2.448	1.701
PBE0	1.829	1.812	1.982	1.682	1.602	2.441	1.701
PBE0-1/3	1.806	1.788	1.956	1.676	1.594	2.442	1.691
M06	1.845	1.831	1.998	1.693	1.608	2.482	1.715
M06HF	1.740	1.731	1.836	1.683	1.575	2.491	1.670
M062X	1.805	1.791	1.944	1.685	1.596	2.469	1.695
ωB97XD	1.815	1.797	1.968	1.680	1.598	2.468	1.694
ωB97X	1.790	1.774	1.930	1.679	1.594	2.481	1.687
ωB97	1.777	1.763	1.907	1.678	1.593	2.498	1.684
LC-ωPBE	1.769	1.754	1.899	1.673	1.587	2.449	1.677
M11	1.796	1.780	1.936	1.679	1.591	2.455	1.683
N12SX	1.802	1.781	1.954	1.674	1.592	2.410	1.685
MN12SX	1.801	1.785	1.958	1.673	1.595	2.479	1.690
M06L	1.903	1.900	2.064	1.700	1.617	2.517	1.738
M11L	1.873	1.874	2.052	1.662	1.588	2.512	1.714
VSXC	1.944	1.938	2.107	1.703	1.622	2.586	1.738
HCTH	1.901	1.892	2.063	1.699	1.618	2.521	1.726
tHCTH	1.907	1.900	2.069	1.699	1.617	2.486	1.729
N12	1.859	1.844	2.006	1.676	1.597	2.419	1.697
MN12L	1.826	1.808	1.995	1.673	1.599	2.529	1.701
B97-D	1.958	1.951	2.112	1.717	1.630	2.523	1.752
B97-D3	1.946	1.942	2.100	1.714	1.629	2.506	1.750
TPSS	1.927	1.922	2.078	1.712	1.629	2.485	1.744
PBE	1.918	1.910	2.062	1.712	1.630	2.465	1.742
BLYP	1.967	1.963	2.114	1.728	1.640	2.530	1.762
LC-BLYP	1.745	1.728	1.867	1.668	1.576	2.456	1.666
APFD	1.918	1.910	2.062	1.712	1.630	2.465	1.742
PBE0-GD3	1.830	1.814	1.984	1.683	1.602	2.443	1.701
PBE0-GD3BJ	1.829	1.812	1.981	1.682	1.602	2.438	1.701
B2PLYP	1.864	1.845	2.034	1.684	1.613	2.487	1.708
B2PLYPD	1.866	1.847	2.037	1.685	1.613	2.483	1.708
MPW2PLYP	1.844	1.824	2.011	1.681	1.607	2.483	1.702
MPW2PLYPD	1.845	1.825	2.013	1.682	1.607	2.480	1.702
ωB97XD*	1.816	1.799	1.968	1.680	1.598	2.464	1.695
ωB97XV*	1.795	1.781	1.932	1.684	1.598	2.466	1.693

* QChem 4.2

Table S16. Energetic parameters (kcal/mol), calculated with different DFT methods (with def2-SV(P)+d basis set).

Method	ΔE(*trans-cis*)	Isomerization $\Delta E^{\neq}$	HSNO D_0(S–N)	N-prot. HSNO		O-prot. HSNO		S-prot. HSNO		Deprot. SNO	
				ΔE(H^+ transf.)	D_0(S–N)	ΔE(H^+ transf.)	D_0(S–N)	ΔE(H^+ transf.)	D_0(S–N)	ΔE(H^+ transf.)	D_0(S–N)
B3LYP	-0.67	11.09	31.02	-3.17	78.44	-1.39	95.46	-12.68	37.43	177.32	56.01
CAM-B3LYP	-0.20	10.72	26.91	-2.93	75.82	-2.65	93.80	-10.01	32.28	174.88	52.69
B3P86	-0.75	11.83	34.81	-2.91	82.08	-0.91	99.34	-9.92	37.66	174.92	59.84
B98	-0.74	11.14	33.13	-2.74	80.35	-1.52	97.50	-11.57	36.85	176.00	57.74
B971	-0.74	11.21	34.52	-2.86	81.31	-1.36	98.64	-11.91	37.29	176.44	58.91
B972	-0.79	11.43	33.24	-3.59	79.93	-1.04	97.01	-13.28	34.96	176.93	57.20
X3LYP	-0.60	11.06	30.94	-3.22	78.64	-1.59	95.65	-12.36	37.36	177.09	56.11
BMK	-0.63	10.69	30.14	-1.54	79.71	-3.76	98.86	-7.55	32.04	171.32	56.80
TPSSh	-1.03	11.45	34.11	-1.67	78.63	1.09	95.31	-12.91	38.58	176.88	57.21
BHandHLYP	-0.22	10.60	18.89	-3.42	69.44	-3.60	85.40	-12.04	28.00	175.64	44.53
tHCTHhyb	-0.87	11.58	36.10	-2.37	81.89	-0.38	98.88	-11.58	38.61	176.25	60.17
PBEh1PBE	-0.62	11.48	32.09	-3.12	79.24	-0.87	96.15	-10.89	35.90	175.14	56.76
PBE0	-0.63	11.55	32.45	-3.14	79.65	-0.95	96.66	-10.58	35.90	175.02	57.11
PBE0-1/3	-0.51	11.37	29.08	-3.24	77.22	-1.63	94.03	-10.32	33.15	174.35	53.99
M06	-0.58	12.03	38.14	-2.25	85.17	-1.42	101.77	-9.89	36.97	176.89	64.51
M06HF	0.20	8.83	23.22	1.77	73.60	-0.14	90.47	-5.67	20.97	166.94	50.99
M062X	-0.29	10.05	29.12	-0.87	77.44	-1.10	95.28	-9.98	29.29	173.05	54.75
ωB97XD	-0.47	10.87	29.81	-3.05	77.45	-2.30	95.49	-11.16	31.21	174.30	54.88
ωB97X	-0.22	10.54	27.49	-2.71	74.98	-2.28	93.37	-11.35	28.57	174.72	52.29
ωB97	-0.09	10.24	25.66	-2.34	72.42	-1.93	90.89	-12.43	26.27	175.29	49.94
LC-ωPBE	-0.12	10.57	23.26	-2.67	71.08	-1.98	89.99	-9.31	25.81	173.42	47.71
M11	-0.02	10.01	27.90	-0.10	75.62	-0.26	92.90	-6.59	26.64	168.22	54.14
N12SX	-0.50	12.41	35.72	-2.78	85.75	-1.88	102.22	-5.22	37.91	172.57	61.59
MN12SX	-0.45	11.72	37.73	0.26	85.35	-1.89	103.17	-5.51	33.07	169.85	65.57
M06L	-1.30	12.81	40.11	-1.16	83.01	2.09	100.25	-12.87	40.78	178.16	62.45
M11L	-1.11	12.73	41.52	-1.27	84.81	-0.09	101.36	-11.86	36.48	176.06	65.63
VSXC	-0.44	11.33	36.25	-1.08	78.42	2.25	95.73	-17.00	39.06	179.95	57.16
HCTH	-1.02	12.93	38.72	-4.00	83.13	1.34	99.70	-14.55	41.78	180.78	61.37
tHCTH	-1.12	12.62	39.65	-2.56	83.40	1.76	99.10	-12.97	42.11	178.80	62.36
N12	-0.94	13.97	45.93	-3.17	93.82	-0.38	109.52	-5.98	45.56	176.21	71.62
MN12L	-0.78	12.33	38.21	2.91	84.91	0.59	101.50	-4.44	34.94	167.05	63.68
B97-D	-0.84	12.11	38.21	-2.13	81.76	2.32	97.54	-14.99	42.66	180.39	60.19
B97-D3	-0.97	12.29	40.10	-2.56	83.99	1.89	99.81	-14.46	43.97	180.45	62.21
TPSS	-1.16	12.09	38.92	-0.86	81.57	2.56	98.33	-12.77	42.11	178.23	61.19
PBE	-0.98	13.12	44.82	-2.00	88.13	2.19	105.26	-10.34	45.13	177.96	68.00
BLYP	-0.92	12.35	39.69	-1.84	83.33	1.44	100.20	-13.07	44.58	180.56	63.07
LC-BLYP	0.35	10.87	24.85	-1.18	74.84	-2.50	94.13	-3.96	27.09	171.52	51.06
APFD	-0.98	13.12	44.82	-2.00	88.13	2.19	105.26	-10.34	45.13	177.96	15.58
PBE0-GD3	-0.53	11.48	32.63	-3.25	79.91	-1.03	96.92	-10.91	36.41	175.13	57.17
PBE0-GD3BJ	-0.61	11.55	33.22	-3.29	80.57	-1.05	97.53	-10.71	36.73	175.17	57.78
B2PLYP	-0.62	10.57	27.17	-3.20	74.79	-1.38	93.84	-14.67	31.30	175.92	53.26
B2PLYPD	-0.49	10.48	27.36	-3.29	75.12	-1.33	94.04	-14.97	31.74	176.00	53.30
MPW2PLYP	-0.48	10.59	26.34	-3.41	74.64	-1.91	93.30	-14.15	30.87	175.76	52.59
MPW2PLYPD	-0.38	10.52	26.47	-3.48	74.87	-1.88	93.45	-14.37	31.19	175.81	52.62
ωB97XD*	-0.46	10.91	29.84	-2.98	77.40	-2.27	95.49	-11.12	31.19	174.33	54.88
ωB97XV*	-0.18	10.23	27.65	-2.74	75.13	-2.39	93.44	-12.00	28.31	175.38	52.04

* QChem 4.2

Table S17. Energetic parameters (kcal/mol), calculated with different DFT methods (with def2-TZVPPD basis set).

Method	ΔE(*trans-cis*)	Isomerization $\Delta E^{\neq}$	HSNO D_0(S–N)	N-prot. HSNO		O-prot. HSNO		S-prot. HSNO		Deprot. SNO	
				ΔE(H^+ transf.)	D_0(S–N)	ΔE(H^+ transf.)	D_0(S–N)	ΔE(H^+ transf.)	D_0(S–N)	ΔE(H^+ transf.)	D_0(S–N)
B3LYP	-1.13	10.49	30.72	-6.35	76.33	-8.25	94.07	-16.44	31.98	167.44	44.92
CAM-B3LYP	-0.82	10.30	26.95	-6.33	74.00	-9.43	92.49	-14.18	27.19	165.99	42.33
B3P86	-1.13	11.22	35.17	-6.15	80.87	-7.91	98.83	-13.53	32.89	166.58	49.86
B98	-1.16	10.52	33.28	-5.26	78.65	-7.92	96.47	-14.58	31.77	166.51	47.24
B971	-1.15	10.60	34.73	-5.45	79.72	-7.88	97.74	-14.81	32.26	166.85	48.63
B972	-1.18	10.93	33.74	-6.04	79.14	-7.58	96.90	-15.54	30.67	167.96	47.63
X3LYP	-1.09	10.47	30.65	-6.31	76.48	-8.35	94.18	-16.01	31.87	167.05	44.95
BMK	-0.98	9.82	30.07	-4.50	76.74	-9.21	96.14	-12.61	25.74	163.45	44.90
TPSSh	-1.33	11.01	34.21	-5.43	78.08	-6.55	95.42	-16.19	34.39	168.39	47.76
BHandHLYP	-0.84	10.21	19.57	-5.38	68.07	-9.08	84.34	-14.76	23.35	166.51	34.32
tHCTHhyb	-1.21	11.04	36.01	-5.52	80.76	-7.45	98.46	-14.63	34.12	167.26	50.15
PBEh1PBE	-1.06	11.00	32.57	-6.08	78.32	-7.71	95.85	-13.69	31.44	166.48	47.07
PBE0	-1.07	11.06	33.01	-5.93	78.68	-7.71	96.34	-13.26	31.40	166.34	47.48
PBE0-1/3	-0.99	10.93	29.97	-5.67	76.52	-7.96	93.84	-12.66	28.90	166.05	44.64
M06	-1.03	10.78	36.81	-4.92	82.25	-7.26	99.64	-14.38	31.14	167.51	50.00
M06HF	-0.45	9.14	25.13	-2.69	74.86	-8.21	92.77	-8.32	18.17	161.10	43.92
M062X	-0.74	9.77	30.13	-4.31	76.64	-8.00	95.07	-13.64	24.43	164.87	45.50
ωB97XD	-0.91	10.25	30.05	-5.75	76.11	-8.42	94.64	-14.53	26.71	165.64	44.09
ωB97X	-0.71	10.08	28.06	-5.86	74.02	-8.74	92.80	-14.92	24.31	166.28	42.97
ωB97	-0.58	9.95	26.37	-6.11	72.13	-9.05	91.03	-16.03	22.60	167.79	41.92
LC-ωPBE	-0.68	10.32	24.29	-6.19	71.08	-8.95	90.34	-12.77	22.49	166.93	40.06
M11	-0.54	9.88	28.80	-5.93	76.57	-9.00	94.40	-12.94	23.71	163.63	45.56
N12SX	-1.06	11.65	35.63	-5.81	83.80	-8.16	100.59	-9.60	32.93	164.83	51.89
MN12SX	-0.99	10.86	35.90	-1.85	81.60	-7.86	99.52	-10.08	27.50	162.12	50.03
M06L	-1.55	11.61	40.00	-5.16	81.76	-5.17	99.84	-18.64	35.36	171.59	50.46
M11L	-1.38	11.31	40.50	-0.80	81.03	-4.75	97.73	-14.09	30.06	164.49	50.10
VSXC	-0.73	10.71	35.01	-5.07	77.14	-5.82	95.36	-20.09	34.26	170.18	47.33
HCTH	-1.31	12.19	38.59	-6.67	81.55	-5.89	98.97	-16.59	36.69	169.48	51.42
tHCTH	-1.38	12.06	39.05	-5.81	82.52	-5.89	99.16	-15.62	38.24	169.23	52.33
N12	-1.38	12.91	44.31	-6.23	90.46	-7.26	106.93	-10.50	39.88	167.07	59.19
MN12L	-1.22	11.15	37.01	0.62	81.86	-5.21	98.53	-8.96	29.43	160.57	48.77
B97-D	-1.08	11.30	37.21	-5.49	79.75	-5.36	96.61	-18.36	37.70	169.87	49.00
B97-D3	-1.23	11.49	39.13	-5.86	82.00	-5.73	98.88	-17.80	39.03	169.91	51.02
TPSS	-1.41	11.53	38.55	-5.18	80.84	-5.71	98.42	-16.52	37.76	169.27	51.45
PBE	-1.28	12.29	44.19	-6.03	86.33	-6.07	104.63	-14.20	39.91	167.91	57.32
BLYP	-1.26	11.46	38.31	-5.98	80.47	-6.56	98.49	-17.62	38.49	169.30	50.88
LC-BLYP	-0.43	10.58	25.21	-5.43	73.42	-9.56	92.95	-9.47	22.53	164.46	41.99
APFD	-1.28	12.29	44.19	-6.03	86.33	-6.07	104.63	-14.20	39.91	167.91	10.08
PBE0-GD3	-0.97	10.99	33.19	-6.04	78.93	-7.80	96.61	-13.61	31.92	166.46	47.53
PBE0-GD3BJ	-1.05	11.05	33.78	-6.08	79.60	-7.81	97.22	-13.41	32.25	166.49	48.14
B2PLYP	-1.08	10.11	29.81	-6.45	75.11	-8.43	94.68	-17.58	26.75	166.38	45.61
B2PLYPD	-0.94	10.02	30.00	-6.55	75.44	-8.41	94.88	-17.91	27.20	166.47	45.65
MPW2PLYP	-1.00	10.16	28.83	-6.37	74.78	-8.65	93.91	-16.88	26.33	166.11	44.66
MPW2PLYPD	-0.91	10.10	28.97	-6.45	75.02	-8.64	94.07	-17.12	26.66	166.18	44.69
ωB97XD*	-0.91	10.29	30.10	-5.67	76.08	-8.38	94.66	-14.47	26.68	165.69	44.10
ωB97XV*	-0.74	9.98	28.73	-5.70	74.73	-9.07	93.59	-14.86	24.24	167.12	43.50

* QChem 4.2

Table S18. Energetic parameters (kcal/mol), calculated with different DFT methods (with aug-pcseg-1 basis set).

Method	ΔE(*trans-cis*)	Isomerization $\Delta E^{\neq}$	HSNO D_0(S–N)	N-prot. HSNO		O-prot. HSNO		S-prot. HSNO		Deprot. SNO	
				ΔE(H^+ transf.)	D_0(S–N)	ΔE(H^+ transf.)	D_0(S–N)	ΔE(H^+ transf.)	D_0(S–N)	ΔE(H^+ transf.)	D_0(S–N)
B3LYP	-1.06	10.15	30.59	-5.32	74.79	-6.86	91.77	-16.89	34.52	167.71	44.52
CAM-B3LYP	-0.78	9.76	26.36	-5.30	72.07	-8.08	89.76	-14.85	29.68	166.14	41.39
B3P86	-1.07	10.82	35.15	-5.47	79.64	-6.89	96.98	-14.63	35.86	167.21	49.52
B98	-1.08	10.13	33.20	-4.45	77.09	-6.57	94.16	-15.37	34.37	166.90	46.88
B971	-1.07	10.20	34.60	-4.62	78.11	-6.51	95.42	-15.72	34.80	167.30	48.15
B972	-1.11	10.43	33.72	-5.49	77.51	-6.46	94.70	-17.15	33.10	168.72	47.38
X3LYP	-1.02	10.10	30.47	-5.25	74.82	-6.92	91.75	-16.52	34.35	167.27	44.53
BMK	-0.97	9.70	29.84	-4.38	76.76	-9.13	95.21	-12.61	29.98	164.28	44.30
TPSSh	-1.23	10.63	34.61	-4.60	76.77	-5.25	93.65	-17.33	36.96	168.92	48.00
BHandHLYP	-0.82	9.50	19.01	-4.65	66.11	-7.84	81.47	-15.89	25.83	166.87	33.44
tHCTHhyb	-1.11	10.65	36.22	-4.70	79.18	-6.20	96.32	-15.76	36.58	167.84	50.07
PBEh1PBE	-1.01	10.45	32.50	-5.31	76.65	-6.48	93.59	-15.23	33.96	167.06	46.66
PBE0	-1.02	10.51	32.93	-5.21	77.07	-6.47	94.10	-14.83	33.96	166.93	47.09
PBE0-1/3	-0.95	10.28	29.82	-5.06	74.84	-6.80	91.52	-14.45	31.52	166.67	44.17
M06	-0.88	10.83	37.06	-6.05	82.43	-8.57	99.37	-15.74	35.28	169.07	51.46
M06HF	-0.35	8.29	24.40	-0.83	71.59	-6.60	88.46	-10.91	20.26	160.03	42.86
M062X	-0.73	9.11	29.73	-2.93	75.00	-6.61	92.69	-14.64	27.64	165.22	44.33
ωB97XD	-0.85	9.80	29.90	-5.65	74.87	-8.08	92.82	-16.15	29.61	166.66	43.88
ωB97X	-0.69	9.52	27.54	-5.54	72.45	-8.20	90.70	-16.63	27.02	167.28	41.99
ωB97	-0.56	9.36	25.70	-5.77	70.34	-8.48	88.77	-18.12	25.10	168.88	40.61
LC-ωPBE	-0.64	9.65	23.61	-5.56	68.99	-7.83	87.62	-14.57	24.71	167.35	38.91
M11	-0.47	9.37	29.21	-5.32	75.51	-8.48	92.87	-13.96	26.90	164.15	45.78
N12SX	-1.02	11.32	35.21	-5.21	82.48	-7.23	98.34	-10.05	35.95	164.97	51.40
MN12SX	-0.87	10.78	38.24	-3.66	83.95	-9.18	101.78	-11.75	32.59	163.53	53.65
M06L	-1.36	11.60	39.83	-6.56	82.79	-6.63	100.71	-19.95	40.24	172.93	51.20
M11L	-1.24	11.23	44.29	-3.09	84.64	-6.81	101.94	-17.15	35.77	167.92	54.74
VSXC	-0.50	10.19	35.55	-3.95	75.36	-4.26	93.13	-21.11	36.09	170.70	47.81
HCTH	-1.25	11.72	38.42	-5.29	79.24	-3.63	96.12	-17.79	38.16	170.02	50.59
tHCTH	-1.26	11.71	39.79	-5.21	81.01	-4.72	97.26	-17.28	40.18	170.11	52.99
N12	-1.23	12.68	43.96	-5.18	88.44	-5.80	103.97	-10.87	42.11	167.08	58.93
MN12L	-1.01	11.21	38.75	-1.61	84.38	-6.80	100.72	-10.30	34.38	161.26	52.18
B97-D	-0.99	11.18	37.86	-4.86	78.79	-4.21	95.12	-19.23	40.00	170.54	49.62
B97-D3	-1.12	11.34	39.74	-5.23	80.99	-4.60	97.37	-18.72	41.36	170.55	51.63
TPSS	-1.29	11.28	39.05	-4.29	79.63	-4.37	96.78	-17.44	40.26	169.73	51.85
PBE	-1.18	12.07	44.33	-5.09	84.99	-4.66	102.71	-15.12	42.28	168.29	57.27
BLYP	-1.16	11.42	38.46	-4.85	79.33	-5.15	96.64	-17.56	40.94	169.30	50.95
LC-BLYP	-0.40	9.94	23.96	-4.35	71.00	-8.20	89.60	-10.13	24.89	164.29	40.27
APFD	-1.18	12.07	44.33	-5.09	84.99	-4.66	102.71	-15.12	42.28	168.29	11.45
PBE0-GD3	-0.92	10.44	33.12	-5.33	77.33	-6.55	94.37	-15.16	34.48	167.04	47.15
PBE0-GD3BJ	-1.00	10.50	33.70	-5.37	77.98	-6.57	94.98	-14.98	34.81	167.07	47.75
B2PLYP	-1.05	9.57	28.87	-5.55	72.59	-7.16	91.49	-19.29	29.31	166.82	43.95
B2PLYPD	-0.93	9.49	29.08	-5.64	72.93	-7.13	91.70	-19.60	29.76	166.93	43.99
MPW2PLYP	-0.98	9.55	27.86	-5.56	72.21	-7.43	90.62	-18.69	28.83	166.52	43.10
MPW2PLYPD	-0.89	9.49	28.01	-5.64	72.46	-7.41	90.78	-18.92	29.16	166.59	43.13
ωB97XD*	-0.86	9.84	29.94	-5.58	74.84	-8.05	92.84	-16.07	29.57	166.71	43.88
ωB97XV*	-0.69	9.33	31.18	-5.04	72.60	-7.91	90.80	-16.49	26.63	167.65	45.51

* QChem 4.2

Table S19. Energetic parameters (kcal/mol), calculated with different DFT methods (with aug-pcseg-2 basis set).

Method	ΔE(*trans-cis*)	Isomeriza-tion $\Delta E^{\neq}$	HSNO D_0(S–N)	N-prot. HSNO		O-prot. HSNO		S-prot. HSNO		Deprot. SNO	
				ΔE(H^+ transf.)	D_0(S–N)	ΔE(H^+ transf.)	D_0(S–N)	ΔE(H^+ transf.)	D_0(S–N)	ΔE(H^+ transf.)	D_0(S–N)
B3LYP	-1.12	10.48	30.65	-6.18	76.36	-8.14	94.11	-16.06	32.14	166.85	45.15
CAM-B3LYP	-0.82	10.26	26.88	-6.12	74.00	-9.31	92.50	-13.77	27.32	165.45	42.46
B3P86	-1.13	11.21	35.14	-5.95	80.92	-7.79	98.90	-13.15	33.08	166.08	49.97
B98	-1.15	10.53	33.21	-5.14	78.72	-7.85	96.56	-14.22	31.93	165.97	47.53
B971	-1.14	10.61	34.65	-5.33	79.79	-7.82	97.84	-14.45	32.40	166.30	48.92
B972	-1.18	10.95	33.68	-5.86	79.19	-7.47	96.99	-15.13	30.86	167.45	47.94
X3LYP	-1.09	10.46	30.59	-6.13	76.50	-8.25	94.22	-15.63	32.03	166.46	45.21
BMK	-0.97	9.80	29.98	-4.29	76.91	-8.99	96.24	-12.18	25.95	162.94	44.65
TPSSh	-1.33	11.02	34.15	-5.27	78.13	-6.45	95.50	-15.85	34.58	167.88	48.14
BHandHLYP	-0.85	10.17	19.63	-5.21	68.13	-8.96	84.40	-14.40	23.47	166.09	34.50
tHCTHhyb	-1.21	11.04	35.88	-5.38	80.75	-7.37	98.47	-14.32	34.27	166.79	50.44
PBEh1PBE	-1.07	11.00	32.55	-5.90	78.39	-7.60	95.94	-13.32	31.59	165.96	47.33
PBE0	-1.08	11.06	32.99	-5.75	78.75	-7.61	96.44	-12.88	31.57	165.82	47.74
PBE0-1/3	-1.00	10.93	30.00	-5.48	76.61	-7.85	93.95	-12.27	29.06	165.58	44.89
M06	-1.02	10.84	36.60	-4.59	82.46	-7.05	99.91	-13.44	31.51	167.07	49.82
M06HF	-0.54	9.07	24.78	-2.68	74.43	-8.28	92.25	-9.13	18.34	160.99	44.18
M062X	-0.76	9.67	30.10	-3.98	76.55	-7.69	94.91	-13.38	24.57	164.43	45.40
ωB97XD	-0.91	10.27	30.05	-5.52	76.24	-8.26	94.83	-14.01	26.92	165.15	44.22
ωB97X	-0.72	10.07	28.01	-5.65	74.06	-8.58	92.89	-14.42	24.46	165.78	42.91
ωB97	-0.58	9.93	26.28	-5.87	72.13	-8.84	91.05	-15.52	22.72	167.35	41.72
LC-ωPBE	-0.69	10.31	24.27	-5.97	71.13	-8.83	90.44	-12.31	22.63	166.46	40.15
M11	-0.57	9.81	28.89	-5.25	76.63	-8.46	94.47	-12.23	23.91	162.90	45.93
N12SX	-1.04	11.70	35.54	-5.63	83.92	-8.08	100.83	-8.94	33.15	164.14	52.14
MN12SX	-1.02	10.94	35.58	-1.48	81.74	-7.55	99.71	-9.15	28.04	161.74	49.84
M06L	-1.55	11.66	39.68	-4.69	81.91	-4.80	100.04	-17.57	35.80	171.09	49.81
M11L	-1.40	11.69	41.19	-0.83	82.73	-4.85	99.36	-13.31	31.32	164.58	50.56
VSXC	-0.72	10.74	34.79	-5.04	77.10	-5.81	95.34	-19.87	34.38	169.66	47.73
HCTH	-1.32	12.24	38.45	-6.62	81.53	-5.89	98.98	-16.33	36.75	168.66	52.17
tHCTH	-1.38	12.10	38.85	-5.70	82.46	-5.82	99.12	-15.31	38.42	168.67	52.87
N12	-1.36	12.98	44.10	-6.16	90.62	-7.23	107.20	-10.00	40.04	166.21	59.82
MN12L	-1.22	11.29	36.72	0.92	82.16	-4.98	98.79	-7.83	29.87	160.04	48.50
B97-D	-1.08	11.33	37.01	-5.33	79.76	-5.25	96.65	-17.96	37.93	169.20	49.35
B97-D3	-1.23	11.52	38.94	-5.70	82.00	-5.62	98.91	-17.40	39.27	169.25	51.37
TPSS	-1.41	11.54	38.44	-5.04	80.87	-5.62	98.48	-16.19	37.96	168.69	51.85
PBE	-1.27	12.31	44.01	-5.90	86.38	-6.01	104.71	-13.84	40.10	167.17	57.66
BLYP	-1.24	11.46	38.13	-5.84	80.50	-6.49	98.54	-17.26	38.68	168.54	51.20
LC-BLYP	-0.43	10.51	25.12	-5.19	73.36	-9.42	92.89	-9.02	22.63	163.93	41.96
APFD	-1.27	12.31	44.01	-5.90	86.38	-6.01	104.71	-13.84	40.10	167.17	11.39
PBE0-GD3	-0.97	10.99	33.17	-5.86	79.01	-7.70	96.71	-13.22	32.08	165.93	47.80
PBE0-GD3BJ	-1.05	11.06	33.77	-5.90	79.67	-7.70	97.32	-13.02	32.41	165.97	48.40
B2PLYP	-1.06	10.21	30.16	-6.47	75.71	-8.52	95.28	-16.99	27.16	165.78	46.44
B2PLYPD	-0.93	10.12	30.35	-6.58	76.03	-8.50	95.48	-17.32	27.62	165.88	46.48
MPW2PLYP	-0.99	10.25	29.18	-6.35	75.34	-8.70	94.48	-16.26	26.72	165.52	45.48
MPW2PLYPD	-0.90	10.19	29.31	-6.43	75.58	-8.69	94.63	-16.50	27.05	165.59	45.51
ωB97XD*	-0.91	10.31	30.10	-5.45	76.22	-8.23	94.85	-13.95	26.90	165.19	44.23
ωB97XV*	-0.74	9.97	28.69	-5.50	74.78	-8.94	93.65	-14.43	24.43	166.64	43.60

* QChem 4.2

Table S20. Performance of DFT functionals, applied to S-N bond lengths (Å).

Method	def2-SV(P)+d		def2-TZVPPD		aug-pcseg-1		aug-pcseg-2	
	RMSD	MAD	RMSD	MAD	RMSD	MAD	RMSD	MAD
B3LYP	0.029	0.069	0.022	0.055	0.031	0.041	0.022	0.055
CAM-B3LYP	0.042	0.064	0.046	0.073	0.027	0.055	0.045	0.074
B3P86	0.017	0.035	0.018	0.031	0.014	0.017	0.017	0.031
B98	0.023	0.058	0.014	0.034	0.025	0.037	0.014	0.033
B971	0.024	0.059	0.013	0.033	0.026	0.038	0.014	0.033
B972	0.027	0.068	0.020	0.036	0.014	0.018	0.020	0.036
X3LYP	0.024	0.061	0.019	0.049	0.026	0.032	0.019	0.049
BMK	0.034	0.057	0.032	0.054	0.018	0.045	0.031	0.053
TPSSh	0.039	0.067	0.020	0.036	0.038	0.059	0.020	0.036
BHandHLYP	0.063	0.092	0.066	0.100	0.043	0.078	0.064	0.100
tHCTHhyb	0.029	0.059	0.012	0.027	0.030	0.048	0.013	0.028
PBEh1PBE	0.024	0.042	0.027	0.044	0.013	0.025	0.027	0.045
PBE0	0.024	0.038	0.028	0.047	0.014	0.027	0.028	0.048
PBE0-1/3	0.040	0.061	0.045	0.074	0.026	0.054	0.044	0.075
M06	0.026	0.051	0.024	0.050	0.019	0.035	0.024	0.045
M06HF	0.098	0.183	0.107	0.201	0.080	0.162	0.102	0.194
M062X	0.044	0.074	0.051	0.090	0.030	0.064	0.048	0.086
ωB97XD	0.040	0.056	0.040	0.061	0.022	0.047	0.039	0.063
ωB97X	0.057	0.090	0.060	0.099	0.041	0.080	0.059	0.100
ωB97	0.068	0.110	0.072	0.122	0.053	0.103	0.071	0.123
LC-ωPBE	0.070	0.118	0.074	0.131	0.056	0.109	0.074	0.132
M11	0.052	0.085	0.057	0.096	0.039	0.077	0.054	0.094
N12SX	0.046	0.075	0.048	0.073	0.036	0.062	0.049	0.076
MN12SX	0.049	0.073	0.050	0.071	0.036	0.064	0.048	0.073
M06L	0.048	0.092	0.044	0.081	0.038	0.055	0.042	0.080
M11L	0.037	0.088	0.037	0.086	0.025	0.045	0.033	0.074
VSXC	0.096	0.154	0.079	0.149	0.093	0.128	0.078	0.149
HCTH	0.061	0.116	0.042	0.084	0.061	0.087	0.041	0.084
tHCTH	0.057	0.085	0.035	0.050	0.055	0.085	0.035	0.049
N12	0.013	0.025	0.013	0.022	0.020	0.030	0.015	0.025
MN12L	0.048	0.108	0.044	0.094	0.026	0.044	0.044	0.091
B97-D	0.088	0.117	0.072	0.101	0.087	0.128	0.071	0.100
B97-D3	0.078	0.106	0.062	0.092	0.079	0.120	0.062	0.091
TPSS	0.068	0.095	0.047	0.072	0.066	0.103	0.047	0.072
PBE	0.056	0.080	0.038	0.060	0.060	0.091	0.038	0.059
BLYP	0.091	0.121	0.079	0.112	0.094	0.137	0.079	0.112
LC-BLYP	0.091	0.158	0.094	0.164	0.075	0.143	0.093	0.163
APFD	0.056	0.080	0.038	0.060	0.060	0.091	0.038	0.059
PBE0-GD3	0.023	0.038	0.027	0.045	0.013	0.026	0.027	0.046
PBE0-GD3BJ	0.023	0.035	0.028	0.048	0.014	0.028	0.028	0.049
B2PLYP	0.031	0.078	0.021	0.053	0.036	0.047	0.019	0.049
B2PLYPD	0.031	0.075	0.020	0.049	0.037	0.049	0.018	0.046
MPW2PLYP	0.029	0.071	0.023	0.049	0.022	0.038	0.023	0.045
MPW2PLYPD	0.028	0.068	0.022	0.046	0.023	0.035	0.022	0.043
ωB97XD*	0.039	0.056	0.038	0.061	0.022	0.046	0.038	0.062
ωB97XV*	0.051	0.083	0.055	0.098	0.037	0.077	0.055	0.099

* QChem 4.2

Table S21. Performance of DFT functionals, applied to energetic parameters (kcal/mol).

Method	def2-SV(P)+d		def2-TZVPPD		aug-pcseg-1		aug-pcseg-2	
	RMSD	MAD	RMSD	MAD	RMSD	MAD	RMSD	MAD
B3LYP	7.33	18.27	4.46	12.82	4.89	15.37	4.52	12.98
CAM-B3LYP	5.53	13.12	3.62	8.03	4.08	10.52	3.70	8.16
B3P86	8.64	18.50	6.03	13.73	6.23	16.71	6.13	13.93
B98	7.71	17.69	4.96	12.61	5.17	15.21	5.06	12.77
B971	8.22	18.13	5.44	13.10	5.54	15.65	5.53	13.25
B972	7.20	15.80	4.79	11.51	4.89	13.95	4.87	11.70
X3LYP	7.33	18.20	4.48	12.72	4.85	15.19	4.54	12.87
BMK	6.71	12.89	3.92	6.58	4.54	10.82	4.10	6.79
TPSSh	7.99	19.42	5.40	15.23	5.86	17.81	5.47	15.42
BHandHLYP	5.42	11.41	5.88	13.27	6.70	14.15	5.86	13.09
tHCTHhyb	8.90	19.45	6.22	14.96	6.34	17.42	6.28	15.11
PBEh1PBE	7.18	16.74	4.82	12.28	4.96	14.80	4.92	12.43
PBE0	7.32	16.74	4.96	12.24	5.07	14.81	5.07	12.41
PBE0-1/3	5.89	14.00	3.98	9.74	4.17	12.37	4.09	9.90
M06	10.10	17.81	6.04	11.98	6.92	16.12	6.21	12.35
M06HF	5.06	11.07	4.29	8.41	4.26	9.42	4.15	8.45
M062X	5.37	10.14	3.18	5.27	3.35	8.48	3.25	5.41
ωB97XD	5.54	12.05	3.47	7.55	3.71	10.46	3.61	7.77
ωB97X	4.49	9.41	2.77	5.15	3.16	7.86	2.89	5.30
ωB97	3.83	7.11	2.57	5.67	3.26	6.97	2.66	5.87
LC-ωPBE	4.21	7.43	3.52	7.52	4.03	8.67	3.59	7.43
M11	5.17	10.14	3.35	5.82	3.37	7.75	3.51	6.55
N12SX	9.98	18.75	7.20	13.77	7.21	16.80	7.40	13.99
MN12SX	10.01	17.99	6.02	9.94	7.57	13.43	6.26	10.08
M06L	10.47	21.62	7.22	16.20	8.59	21.08	7.27	16.64
M11L	10.36	18.05	6.22	10.90	8.70	16.61	6.99	12.16
VSXC	8.56	19.90	5.40	15.10	5.75	16.93	5.39	15.22
HCTH	10.47	22.62	7.25	17.53	7.04	19.00	7.29	17.59
tHCTH	10.60	22.95	7.81	19.09	8.02	21.02	7.86	19.26
N12	15.38	26.40	11.48	20.72	11.13	22.95	11.64	20.88
MN12L	10.21	16.09	6.71	10.27	8.05	15.22	7.03	10.71
B97-D	10.21	23.50	6.80	18.54	7.31	20.84	6.84	18.78
B97-D3	11.20	24.81	7.83	19.87	8.25	22.20	7.87	20.11
TPSS	10.22	22.95	7.30	18.60	7.72	21.10	7.37	18.80
PBE	13.52	25.97	10.26	20.75	10.32	23.12	10.34	20.94
BLYP	11.39	25.42	7.39	19.33	7.74	21.78	7.44	19.52
LC-BLYP	5.48	12.78	3.91	7.26	4.29	7.31	4.05	7.72
APFD	15.42	32.00	14.98	37.51	14.72	36.13	14.72	36.19
PBE0-GD3	7.46	17.25	5.12	12.76	5.24	15.32	5.23	12.92
PBE0-GD3BJ	7.75	17.57	5.40	13.09	5.47	15.65	5.50	13.25
B2PLYP	5.14	12.14	3.16	7.59	3.51	10.15	3.40	8.00
B2PLYPD	5.26	12.58	3.31	8.04	3.65	10.60	3.56	8.46
MPW2PLYP	4.94	11.71	3.07	7.17	3.50	9.67	3.27	7.57
MPW2PLYPD	5.02	12.03	3.17	7.50	3.58	10.00	3.36	7.90
ωB97XD*	5.55	12.03	3.46	7.53	3.69	10.41	3.60	7.74
ωB97XV*	4.41	9.16	2.72	5.08	2.47	7.47	2.81	5.28

* QChem 4.2

Table S22. Performance of DFT functionals, applied to harmonic vibrational frequencies of *cis*- and *trans*-HSNO (cm^{-1}).

Method	def2-SV(P)+d		def2-TZVPPD		aug-pcseg-1		aug-pcseg-2	
	RMSD	MAD	RMSD	MAD	RMSD	MAD	RMSD	MAD
B3LYP	71.4	166.2	35.6	77.6	50.5	115.0	35.8	75.9
CAM-B3LYP	78.2	171.7	44.8	87.3	55.1	126.1	44.3	86.5
B3P86	76.0	183.9	39.9	94.7	54.5	131.4	39.5	93.4
B98	75.9	169.3	38.5	82.5	54.6	124.1	38.5	81.1
B971	74.4	167.0	36.8	78.2	53.2	120.7	36.9	76.6
B972	82.9	204.0	47.8	112.4	65.1	154.6	46.9	111.1
X3LYP	72.0	169.4	35.0	79.9	50.4	118.1	35.2	78.4
BMK	95.2	166.6	63.0	125.2	88.4	173.3	60.0	116.6
TPSSh	72.1	171.1	36.1	72.3	51.3	110.6	35.2	70.2
BHandHLYP	112.6	231.9	83.3	153.8	92.9	190.4	82.3	153.2
tHCTHhyb	77.5	170.8	40.0	79.2	55.2	118.0	40.2	78.3
PBEh1PBE	83.9	202.8	47.1	109.8	62.9	151.2	46.5	108.2
PBE0	83.8	201.8	47.1	109.0	63.3	151.6	46.6	107.5
PBE0-1/3	95.7	220.4	62.2	131.4	76.9	173.5	61.5	130.5
M06	84.6	194.2	55.4	131.0	60.3	140.7	54.1	125.7
M06HF	131.0	253.9	115.3	163.0	105.5	190.5	110.5	161.0
M062X	94.3	207.8	60.0	119.7	71.9	163.6	58.5	120.3
ωB97XD	79.3	181.4	46.2	98.3	59.2	137.1	46.1	98.6
ωB97X	91.9	185.6	62.7	104.8	72.3	143.0	62.2	105.3
ωB97	102.5	193.1	76.2	109.0	84.7	144.7	75.4	110.4
LC-ωPBE	104.2	202.3	76.8	122.4	86.9	157.6	76.1	121.2
M11	90.9	186.0	62.4	106.5	63.9	133.0	59.5	103.6
N12SX	79.5	175.4	47.7	94.0	59.8	128.8	47.6	93.0
MN12SX	76.7	164.5	48.2	89.7	55.1	109.4	48.3	90.7
M06L	84.5	204.4	61.6	136.3	63.2	144.6	58.4	131.3
M11L	109.5	259.9	85.6	205.0	93.5	215.7	84.4	206.3
VSXC	94.6	206.5	56.6	99.5	77.8	142.9	55.7	98.4
HCTH	89.9	207.3	55.0	107.1	75.8	159.3	53.6	104.1
tHCTH	88.1	193.3	54.2	97.4	68.0	134.6	53.3	95.6
N12	71.2	166.3	37.3	74.2	51.2	111.5	36.8	74.2
MN12L	77.7	178.5	50.5	109.9	57.4	122.8	49.9	108.7
B97-D	88.1	171.7	59.3	86.9	68.9	114.4	59.4	85.9
B97-D3	87.8	167.4	60.1	102.7	70.3	112.3	60.3	101.8
TPSS	76.0	147.4	47.4	89.6	56.8	99.4	47.4	89.3
PBE	83.7	144.7	56.3	97.0	64.7	106.1	56.9	96.3
BLYP	92.1	161.2	71.5	121.6	79.6	130.4	73.3	121.8
LC-BLYP	120.1	216.9	93.2	139.2	97.2	171.3	91.6	138.2
APFD	83.7	144.7	56.3	97.0	64.7	106.1	56.9	96.3
PBE0-GD3	84.0	201.8	47.2	109.6	63.5	152.2	46.6	108.0
PBE0-GD3BJ	83.9	201.9	47.2	108.9	63.3	151.5	46.6	107.4
B2PLYP	44.4	107.3	16.5	34.4	31.7	49.2	13.2	27.8
B2PLYPD	45.2	108.7	15.6	34.3	31.0	51.1	12.4	27.7
MPW2PLYP	50.4	121.8	16.1	26.6	31.9	65.4	13.3	22.8
MPW2PLYPD	51.0	122.7	16.0	25.0	31.9	66.5	13.5	22.0
ωB97XD*	81.7	182.2	48.5	102.5	61.0	137.0	48.2	102.2
ωB97XV*	83.9	173.7	54.9	91.8	65.5	131.9	54.4	91.1

* QChem 4.2

Bibliography

1. Adler, T. B., Knizia, G., & Werner, H. -J. (2007). A simple and efficient CCSD (T)-F12 approximation. *The Journal of Chemical Physics*, *127*(22), 221106.

2. Anand, P., & Stamler, J. S. (2012). Enzymatic mechanisms regulating protein *S*-nitrosylation: Implications in health and disease. *Journal of Molecular Medicine*, *90*(3), 233-244.

3. Anand, P., Hess, D. T., & Stamler, J. S. (2013). Identifying single *S*-nitrosothiol sites with cardioprotection. *Circulation Research*, *113*(7), 849-51.

4. Baciu, C., & Gauld, J. W. (2003). An assessment of theoretical methods for the calculation of accurate structures and S-N bond dissociation energies of *S*-nitrosothiols (RSNOs). *The Journal of Physical Chemistry A*, *107*(46), 9946-9952.

5. Baker, J. (1986). An algorithm for the location of transition states. *Journal of Computational Chemistry*, *7*(4), 385-395.

6. Banerjee, A., Adams, N., Simons, J., & Shepard, R. (1985). Search for stationary points on surfaces. *The Journal of Physical Chemistry*, *89*(1), 52-57.

7. Bartberger, M. D., Mannion, J. D., Powell, S. C., Stamler, J. S., Houk, K. N., & Toone, E. J. (2001). S-N dissociation energies of *S*-nitrosothiols: On the origins of nitrosothiol decomposition rates. *Journal of the American Chemical Society*, *123*(36), 8868-8869.

8. Becke, A. D. (2014). Perspective: Fifty years of density-functional theory in chemical physics. *The Journal of Chemical Physics*, *140*(18), 18A301.

9. Billeter, S. R., Turner, A. J., & Thiel, W. (2000). Linear scaling geometry optimisation and transition state search in hybrid delocalised internal coordinates. *Physical Chemistry Chemical Physics*, *2*(10), 2177-2186.

10. Binkley, J. S., Pople, J. A., & Hehre, W. J. (1980). Self-consistent molecular orbital methods. 21. Small split-valence basis sets for first-row elements. *Journal of the American Chemical Society*, *102*(3), 939-947.

11. Bruce King, S. (2012). Potential biological chemistry of hydrogen sulfide (H_2S) with the nitrogen oxides. *Free Radical Biology and Medicine.*

12. Burke, K. (2012). Perspective on density functional theory. *The Journal of Chemical Physics*, *136*(15), 150901.

13. Cerjan, C. J., & Miller, W. H. (1981). On finding transition states. *The Journal of Chemical Physics*, *75*(6), 2800-2806.

14. Cox, A. G., Saunders, D. C., Kelsey, P. B., Conway, A. A., Tesmenitsky, Y., Marchini, J. F., . . . Goessling, W. (2014). S-nitrosothiol signaling regulates liver development and improves outcome following toxic liver injury. *Cell Reports*, *6*(1), 56-69.

15. Dixon, D. A., Feller, D., Peterson, K. A., Wheeler, R. A., & Tschumper, G. S. (2012). A practical guide to reliable first principles computational thermochemistry predictions across the periodic table. *Annual Reports in Computational Chemistry*, *8*, 1-28.

16. Doulias, P. T., Greene, J. L., Greco, T. M., Tenopoulou, M., Seeholzer, S. H., Dunbrack, R. L., & Ischiropoulos, H. (2010). Structural profiling of endogenous S-nitrosocysteine residues reveals unique features that accommodate diverse mechanisms for protein s-nitrosylation. *Proceedings of the National Academy of Sciences of the United States of America*, *107*(39), 16958-63.

17. Dunning Jr, T. H., Peterson, K. A., & Wilson, A. K. (2001). Gaussian basis sets for use in correlated molecular calculations. X. The atoms aluminum through argon revisited. *The Journal of Chemical Physics*, *114*(21), 9244-9253.

18. Easton, R. E., Giesen, D. J., Welch, A., Cramer, C. J., & Truhlar, D. G. (1996). The MIDI! Basis set for quantum mechanical calculations of molecular geometries and partial charges. *Theoretica Chimica Acta*, *93*(5), 281-301.

19. Feller, D. (1996). The role of databases in support of computational chemistry calculations. *Journal of Computational Chemistry*, *17*(13), 1571-1586.

20. Filipovic, M. R., Miljkovic, J. L. j., Nauser, T., Royzen, M., Klos, K., Shubina, T., Ivanović-Burmazović, I. (2012). Chemical characterization of the smallest s-nitrosothiol, HSNO; cellular cross-talk of H_2S and S-nitrosothiols. *Journal of the American Chemical Society*, *134*(29), 12016-27.

21. Francl, M. M., Pietro, W. J., Hehre, W. J., Binkley, J. S., Gordon, M. S., DeFrees, D. J., & Pople, J. A. (1982). Self-consistent molecular orbital methods. XXIII. A polarization-type basis set for second-row elements. *The Journal of Chemical Physics*, *77*(7), 3654-3665.

22. Frisch, M., Trucks, G. W., Schlegel, H. B., Scuseria, G. E., Robb, M. A., Cheeseman, J. R., Petersson, G. A. (2009). Gaussian 09, gaussian. *Inc., Wallingford, CT*.

23. *Gaussian Basis Sets for Molecular Calculations.* (1984). *Gaussian basis sets for molecular calculations.* Amsterdam ; New York: Elsevier ; New York.

24. Gordon, M. S., Binkley, J. S., Pople, J. A., Pietro, W. J., & Hehre, W. J. (1982). Self-consistent molecular-orbital methods. 22. Small split-valence basis sets for second-row elements. *Journal of the American Chemical Society*, *104*(10), 2797-2803.

25. Haldar, S. M., & Stamler, J. S. (2013). S-nitrosylation: Integrator of cardiovascular performance and oxygen delivery. *The Journal of Clinical Investigation*, *123*(1), 101-10.

26. Hampel, C., Peterson, K. A., & Werner, H. -J. (1992). A comparison of the efficiency and accuracy of the quadratic configuration interaction (QCISD), coupled cluster (CCSD), and brueckner coupled cluster (BCCD) methods. *Chemical Physics Letters*, *190*(1), 1-12.

27. Hehre, W. J., Ditchfield, R., & Pople, J. A. (2003). Selfconsistent molecular orbital methods. XII. Further extensions of gaussiantype basis sets for use in molecular orbital studies of organic molecules. *The Journal of Chemical Physics*, *56*(5), 2257-2261.

28. Heinrich, T. A., daSilva, R. S., Miranda, K. M., Switzer, C. H., Wink, D. A., & Fukuto, J. M. (2013). Biological nitric oxide signaling: Chemistry and terminology (NO chemical biology and terminology). *British Journal of Pharmacology.*

29. Hess, D. T., & Stamler, J. S. (2012). Regulation by S-nitrosylation of protein post-translational modification. *Journal of Biological Chemistry*, *287*(7), 4411-4418.

30. Hill, J. G., Mazumder, S., & Peterson, K. A. (2010). Correlation consistent basis sets for molecular core-valence effects with explicitly correlated wave functions: The atoms B-Ne and Al-Ar. *The Journal of Chemical Physics*, *132*(5), 054108.

31. Hill, J. G., Peterson, K. A., Knizia, G., & Werner, H. J. (2009). Extrapolating MP2 and CCSD explicitly correlated correlation energies to the complete basis set limit with first and second row correlation consistent basis sets. *The Journal of Chemical Physics*, *131*(19), 194105.

32. Hochlaf, M., Linguerri, R., & Francisco, J. S. (2013). On the role of the simplest S-nitrosothiol, HSNO, in atmospheric and biological processes. *The Journal of Chemical Physics*, *139*(23), 234304.

33. Hrenar, T., Werner, H. J., & Rauhut, G. (2007). Accurate calculation of anharmonic vibrational frequencies of medium sized molecules using local coupled cluster methods. *The Journal of Chemical Physics*, *126*(13), 134108.

34. Ivanova, L. V., Anton, B. J., & Timerghazin, Q. K. (2014). On the possible biological relevance of HSNO isomers: A computational investigation. *Physical Chemistry Chemical Physics, 16,* 8476-8486.

35. Janssen, C. L., & Nielsen, I. (1998). New diagnostics for coupled-cluster and Møller-Plesset perturbation theory. *Chemical Physics Letters*, *290*(4), 423-430.

36. Jensen, F. (2014). Unifying general and segmented contracted basis sets. Segmented polarization consistent basis sets. *Journal of Chemical Theory and Computation, 135,* 144116.

37. Kästner, J., Carr, J. M., Keal, T. W., Thiel, W., Wander, A., & Sherwood, P. (2009). DL-FIND: An open-source geometry optimizer for atomistic simulations. *The Journal of Physical Chemistry. A*, *113*(43), 11856-65.

38. Kendall, R. A., Dunning, T. H., & Harrison, R. J. (1992). Electron affinities of the first-row atoms revisited. Systematic basis sets and wave functions. *The Journal of Chemical Physics*, *96*(9), 6796-6806.

39. Klimeš, J., & Michaelides, A. (2012). Perspective: Advances and challenges in treating van der waals dispersion forces in density functional theory. *The Journal of Chemical Physics*, *137*(12), 120901.

40. Knizia, G., Adler, T. B., & Werner, H. -J. (2009). Simplified CCSD (T)-F12 methods: Theory and benchmarks. *The Journal of Chemical Physics*, *130*(5), 054104.

41. Krylov, A. I., & Gill, P. M. (2013). Q-Chem: An engine for innovation. *Wiley Interdisciplinary Reviews: Computational Molecular Science*, *3*(3), 317-326.

42. K´allay, M. (n.d.). *MRCC, a string-based quantum chemical program suite*.

43. Lee, T. J., & Taylor, P. R. (1989). A diagnostic for determining the quality of single-reference electron correlation methods. *International Journal of Quantum Chemistry*, *36*(S23), 199-207.

44. Liu, D. C., & Nocedal, J. (1989). On the limited memory BFGS method for large scale optimization. *Mathematical Programming*, *45*(1-3), 503-528.

45. Marchetti, O., & Werner, H. J. (2008). Accurate calculations of intermolecular interaction energies using explicitly correlated wave functions. *Physical Chemistry Chemical Physics : PCCP*, *10*(23), 3400-9.

46. Mardirossian, N., & Head-Gordon, M. (2014). ΩB97X-V: A 10-parameter, range-separated hybrid, generalized gradient approximation density functional with nonlocal correlation, designed by a survival-of-the-fittest strategy. *Physical Chemistry Chemical Physics : PCCP*, *16*(21), 9904-24.

47. Martin, J. M., & Kesharwani, M. K. (2014). Assessment of CCSD (T)-F12 approximations and basis sets for harmonic vibrational frequencies. *Journal of Chemical Theory and Computation.*

48. Miljkovic, J., Eberhardt, M., Herrmann, M., Messlinger, K., Reeh, P., Ivanovic-Burmazovic, I., & Filipovic, M. R. (2013). PL13 saying NO to H_2S. *Nitric Oxide : Biology and Chemistry / Official Journal of the Nitric Oxide Society*, *31*(Supplement 2).

49. Moran, E. E., Timerghazin, Q. K., Kwong, E., & English, A. M. (2011). Kinetics and mechanism of s-nitrosothiol acid-catalyzed hydrolysis: Sulfur activation promotes facile NO^+ release. *The Journal of Physical Chemistry. B*, *115*(12), 3112-26.

50. Neff, M., & Rauhut, G. (2009). Toward large scale vibrational configuration interaction calculations. *The Journal of Chemical Physics*, *131*(12), 124129.

51. Nocedal, J. (1980). Updating quasi-newton matrices with limited storage. *Mathematics of Computation*, *35*(151), 773-782.

52. Nonella, M., Huber, J. R., & Ha, T. K. (1987). Photolytic preparation and isomerization of thionyl imide, thiocyanic acid, thionitrous acid, and nitrogen hydroxide sulfide in an argon matrix: An experimental and theoretical study. *Journal of Physical Chemistry*, *91*(20), 5203-5209.

53. Papajak, E., & Truhlar, D. G. (2010). Convergent partially augmented basis sets for post-hartree- fock calculations of molecular properties and reaction barrier heights. *Journal of Chemical Theory and Computation*, *7*(1), 10-18.

54. Papajak, E., Zheng, J., Xu, X., Leverentz, H. R., & Truhlar, D. G. (2011). Perspectives on basis sets beautiful: Seasonal plantings of diffuse basis functions. *Journal of Chemical Theory and Computation*, *7*(10), 3027-3034.

55. Perissinotti, L. L., Estrin, D. A., Leitus, G., & Doctorovich, F. (2006). A surprisingly stable S-nitrosothiol complex. *Journal of the American Chemical Society*, *128*(8), 2512-3.

56. Peterson, K. A., Adler, T. B., & Werner, H. J. (2008). Systematically convergent basis sets for explicitly correlated wavefunctions: The atoms H, He, B-Ne, and Al-Ar. *The Journal of Chemical Physics*, *128*(8), 084102.

57. Peterson, K. A., Feller, D., & Dixon, D. A. (2012). Chemical accuracy in *ab initio* thermochemistry and spectroscopy: Current strategies and future challenges. *Theoretical Chemistry Accounts*, *131*(1), 1-20.

58. Quiroga, S. L., Almaraz, A. E., Amorebieta, V. T., Perissinotti, L. L., & Olabe, J. A. (2011). Addition and redox reactivity of hydrogen sulfides (H_2S/HS^-) with ni-

troprusside: New chemistry of nitrososulfide ligands. *Chemistry (Weinheim An Der Bergstrasse, Germany)*, *17*(15), 4145-56.

59. Raghavachari, K., Trucks, G. W., Pople, J. A., & Head-Gordon, M. (1989). A fifth-order perturbation comparison of electron correlation theories. *Chemical Physics Letters*, *157*(6), 479-483.

60. Raju, K., Doulias, P. T., Tenopoulou, M., Greene, J. L., & Ischiropoulos, H. (2012). Strategies and tools to explore protein s-nitrosylation. *Biochimica Et Biophysica Acta*, *1820*(6), 684-8.

61. Rappoport, D., & Furche, F. (2010). Property-optimized gaussian basis sets for molecular response calculations. *The Journal of Chemical Physics*, *133*(13), 134105.

62. Rauhut, G. (2004). Efficient calculation of potential energy surfaces for the generation of vibrational wave functions. *The Journal of Chemical Physics*, *121*(19), 9313-9322.

63. Rauhut, G., & Hrenar, T. (2008). A combined variational and perturbational study on the vibrational spectrum of P_2F_4. *Chemical Physics*, *346*(1), 160-166.

64. Schäfer, A., Horn, H., & Ahlrichs, R. (1992). Fully optimized contracted gaussian basis sets for atoms Li to Kr. *The Journal of Chemical Physics*, *97*(4), 2571-2577.

65. Schuchardt, K. L., Didier, B. T., Elsethagen, T., Sun, L., Gurumoorthi, V., Chase, J., Windus, T. L. (2007). Basis set exchange: A community database for computational sciences. *J Chem Inf Model*, *47*(3), 1045-52.

66. Shao, Y., Molnar, L. F., Jung, Y., Kussmann, J., Ochsenfeld, C., Brown, S. T., Head-Gordon, M. (2006). Advances in methods and algorithms in a modern quantum chemistry program package. *Physical Chemistry Chemical Physics : PCCP*, *8*(27), 3172-91.

67. Simons, J., Joergensen, P., Taylor, H., & Ozment, J. (1983). Walking on potential energy surfaces. *The Journal of Physical Chemistry*, *87*(15), 2745-2753.

68. Stanton, J. F., Gauss, J., Harding, M. E., Szalay, P. G., Auer, A. A., Bartlett, R. J., Bomble, Y. J. (2009). CFOUR, a quantum chemical program package.

69. Talipov, M. R., & Timerghazin, Q. K. (2013). Protein control of S-nitrosothiol reactivity: Interplay of antagonistic resonance structures. *The Journal of Physical Chemistry. B*, *117*(6), 1827-37.

70. Talipov, M. R., Khomyakov, D. G., Xian, M., & Timerghazin, Q. K. (2013). Computational design of s-nitrosothiol "click" reactions. *Journal of Computational Chemistry*, *34*(18), 1527-30.

71. Timerghazin, Q. K., & Talipov, M. R. (2013). Unprecedented external electric field effects on S-nitrosothiols: Possible mechanism of biological regulation? *The Journal of Physical Chemistry Letters*, *4*(6), 1034-1038.

72. Timerghazin, Q. K., Peslherbe, G. H., & English, A. M. (2007). Resonance description of S-nitrosothiols: Insights into reactivity. *Org Lett*, *9*(16), 3049-52.

73. Timerghazin, Q. K., Peslherbe, G. H., & English, A. M. (2008). Structure and stability of HSNO, the simplest S-nitrosothiol. *Physical Chemistry Chemical Physics*, *10*(11), 1532-1539.

74. Wang, N. X., & Wilson, A. K. (2005). Density functional theory and the correlation consistent basis sets: The tight d effect on HSO and HOS. *The Journal of Physical Chemistry. A*, *109*(32), 7187-96.

75. Weigend, F., & Ahlrichs, R. (2005). Balanced basis sets of split valence, triple zeta valence and quadruple zeta valence quality for H to Rn: Design and assessment of accuracy. *Physical Chemistry Chemical Physics*, *7*(18), 3297-3305.

76. Werner, H. -, Knowles, P. J., Knizia, G., Manby, F. R., & Schütz, M. (2012). Molpro: A general multipurpose quantum chemistry program package. *WIREs Comput Mol Sci*, *2*, 242-253.